arXiv:2201.05537v2 [hep-ph] 8 Mar 2022

Visible energy and angular distributions of the charged particle from the $\tau-$decay in $b \to c\tau\,(\mu\bar{\nu}_\mu\nu_\tau, \pi\nu_\tau, \rho\nu_\tau)\bar{\nu}_\tau$ reactions

Neus Penalva,[1] Eliecer Hernández,[2] and Juan Nieves[1]

[1] *Instituto de Física Corpuscular (centro mixto CSIC-UV), Institutos de Investigación de Paterna, C/Catedrático José Beltrán 2, E-46980 Paterna, Valencia, Spain*

[2] *Departamento de Física Fundamental e IUFFyM, Universidad de Salamanca, Plaza de la Merced s/n, E-37008 Salamanca, Spain*

(Dated: March 9, 2022)

We study the $d^2\Gamma_d/(d\omega d\cos\theta_d)$, $d\Gamma_d/d\cos\theta_d$ and $d\Gamma_d/dE_d$ distributions, which are defined in terms of the visible energy and polar angle of the charged particle from the $\tau-$decay in $b \to c\tau\,(\mu\bar{\nu}_\mu\nu_\tau, \pi\nu_\tau, \rho\nu_\tau)\bar{\nu}_\tau$ reactions. These differential decay widths could be measured in the near future with certain precision. The first two contain information on the transverse tau-spin, tau-angular and tau-angular-spin asymmetries of the $H_b \to H_c\tau\bar{\nu}_\tau$ parent decay and, from a dynamical point of view, they are richer than the commonly used one, $d^2\Gamma_d/(d\omega dE_d)$, since the latter only depends on the tau longitudinal polarization. We pay attention to the deviations with respect to the predictions of the standard model (SM) for these new observables, considering new physics (NP) operators constructed using both right- and left-handed neutrino fields, within an effective field-theory approach. We present results for $\Lambda_b \to \Lambda_c\tau\,(\mu\bar{\nu}_\mu\nu_\tau, \pi\nu_\tau, \rho\nu_\tau)\bar{\nu}_\tau$ and $\bar{B} \to D^{(*)}\tau\,(\mu\bar{\nu}_\mu\nu_\tau, \pi\nu_\tau, \rho\nu_\tau)\bar{\nu}_\tau$ sequential decays and discuss their use to disentangle between different NP models. In this respect, we show that $d\Gamma_d/d\cos\theta_d$, which should be measured with sufficiently good statistics, becomes quite useful, especially in the $\tau \to \pi\nu_\tau$ mode. The study carried out in this work could be of special relevance due to the recent LHCb measurement of the lepton flavor universality ratio $\mathcal{R}_{\Lambda_c}$ in agreement with the SM. The experiment identified the τ using its hadron decay into $\pi^-\pi^+\pi^-\nu_\tau$, and this result for $\mathcal{R}_{\Lambda_c}$, which is in conflict with the phenomenology from the b-meson sector, needs confirmation from other tau reconstruction channels.

I. INTRODUCTION

In the quest to discover new physics (NP) beyond the Standard Model (SM), the experimental signals of possible violations of lepton flavor universality (LFU) in charged-current (CC) semileptonic $B \to D^{(*)}$ decays reported by BaBar [1, 2], Belle [3–6] and LHCb [7–9] have triggered a large activity in recent years. These experiments measured the $\mathcal{R}_D = \Gamma(\bar{B} \to D\tau\bar{\nu}_\tau)/\Gamma(\bar{B} \to D\ell\bar{\nu}_\ell)$ and $\mathcal{R}_{D^*} = \Gamma(\bar{B} \to D^*\tau\bar{\nu}_\tau)/\Gamma(\bar{B} \to D^*\ell\bar{\nu}_\ell)$ ratios ($\ell = e, \mu$), which combined analysis give rise to a 3.1σ tension with SM results [10]. The similar $\mathcal{R}_{J/\psi} = \Gamma(\bar{B}_c \to J/\psi\tau\bar{\nu}_\tau)/\Gamma(\bar{B}_c \to J/\psi\mu\bar{\nu}_\mu)$ observable, measured by the LHCb Collaboration [11], provides also a 1.8 σ discrepancy with different SM predictions [12–24]. Belle has also provided results for the averaged tau-polarization asymmetry and the longitudinal D^* polarization [5, 25], which together with an upper bound of the leptonic decay rate $\bar{B}_c \to \tau\bar{\nu}_\tau$ [26], are commonly used to constrain NP contributions in the theoretical global fits to these LFU anomalies.

Another reaction that could shed light on the $\mathcal{R}_{D^{(*)}}$ puzzle is the $\Lambda_b \to \Lambda_c\tau\bar{\nu}_\tau$ decay, and in particular the universality ratio $\mathcal{R}_{\Lambda_c}$ can be analogously constructed. A result of $\mathcal{R}_{\Lambda_c} = 0.242 \pm 0.026 \pm 0.040 \pm 0.059$ has just been announced by the LHCb collaboration [27], which is in agreement within errors with the SM prediction ($\mathcal{R}^{\rm SM}_{\Lambda_c} = 0.332 \pm 0.007 \pm 0.007$ [28]). Contrary, to what is found for the ratios measured for the $b \to c$ transitions in the meson sector, the central value reported in [27] turns out to be below the SM result. The τ^- lepton in [27] is reconstructed using the three-prong hadronic $\tau^- \to \pi^-\pi^+\pi^-(\pi^0)\,\nu_\tau$ decay, with the same technique used by the LHCb experiment to obtain the $\mathcal{R}_{D^*} = 0.291 \pm 0.019 \pm 0.026 \pm 0.013$ measurement [9], which is only 1σ higher than the SM prediction. We notice that LHCb reported a significant higher value for $\mathcal{R}_{D^*}$ ($0.336 \pm 0.027 \pm 0.030$), 2.1σ higher than that expected from LFU in the SM, when the τ lepton was reconstructed using its leptonic decay into a muon [7].

One expects that the existence of NP that leads to LFU violation in semitauonic $b-$meson decays would also affect the $\Lambda_b \to \Lambda_c\tau\bar{\nu}_\tau$ reaction, and thus, a confirmation of the result of Ref. [27] for $\mathcal{R}_{\Lambda_c}$, using other reconstruction channels will shed light into this puzzling situation. Such research might provide very stringent constraints on NP extensions of the SM, since scenarios leading to different deviations from SM expectations for $\mathcal{R}_{\Lambda_c}$ and $\mathcal{R}_{D^{(*)}}$ seem to be required. A new measurement of $\mathcal{R}_{\Lambda_c}$, through the $\tau \to \mu\nu_\tau\bar{\nu}_\mu$ decay channel, is in progress at the LHCb experiment [29], which in light of the previous discussion will undoubtedly be very relevant.

As we will detail below, we present in this work some energy and angular distributions of a charged particle product from the decay of the τ produced in the $b \to c\tau\bar{\nu}_\tau$ transition that, if measured, could contribute significantly to clarify the current situation regarding the violation of universality in $b-$hadron decays.

There is a multitude of theoretical works evaluating NP effects on the LFU ratios and on the outgoing unpolarized (or longitudinally polarized) tau angular distributions in $\bar{B} \to D^{(*)}$ [30–50], $\bar{B}_c \to J/\psi, \eta_c$ [20, 22, 50–52] or $\Lambda_b \to \Lambda_c$ [39, 42, 49, 53–65] semileptonic decays. In general, different NP scenarios usually lead to an equally good reproduction of the LFU ratios, and hence other observables are needed to constrain and determine the most plausible NP extension of the SM. Typically, the τ forward-backward (A_{FB}) and longitudinal polarization ($\mathcal{A}_{\lambda_\tau} = \langle P_L^{\rm CM}\rangle$) asymmetries turn out to be more convenient for this purpose[1]. The final τ does not travel far enough for a displaced vertex, and it is very difficult to reconstruct from its decay products since they involve at least one more neutrino. Thus, the maximal accessible information on the $b \to c\tau\bar{\nu}_\tau$ transition is encoded in the visible [66–68] decay products of the τ lepton, for which the three dominant modes $\tau \to \pi\nu_\tau$, $\rho\nu_\tau$ and $\ell\bar{\nu}_\ell\nu_\tau$ ($\ell = e, \mu$) account for more than 70% of the total τ decay width (Γ_τ).

[1] A greater discriminating power can be also reached by analyzing the four-body $\bar{B} \to D^*(D\pi, D\gamma)\tau\bar{\nu}_\tau$ [33–36, 41, 45, 48] or similarly in the baryon reaction by considering the $\Lambda_c \to \Lambda\pi$ decay [61, 63].

For the subsequent decays of the produced τ, after the $b \to c\tau\bar{\nu}_\tau$ transition,

$$H_b \to H_c \tau^- \bar{\nu}_\tau$$
$$\hookrightarrow \pi^- \nu_\tau,\, \rho^- \nu_\tau,\, \mu^- \bar{\nu}_\mu \nu_\tau.\, e^- \bar{\nu}_e \nu_\tau, \tag{1}$$

we have [69] (the expression below was derived in Refs. [66–68] for the particular case of $\bar{B} \to D^{(*)}$ decays)

$$\frac{d^3\Gamma_d}{d\omega d\xi_d d\cos\theta_d} = \mathcal{B}_d \frac{d\Gamma_{\rm SL}}{d\omega}\Big\{F_0^d(\omega,\xi_d) + F_1^d(\omega,\xi_d)\cos\theta_d + F_2^d(\omega,\xi_d)P_2(\cos\theta_d)\Big\}, \tag{2}$$

where all involved kinematical variables are shown in Fig. 1. In Eq. (2), ω is the product of the two hadron four-velocities which is related to the four-momentum transferred as $q^2 = (p-p')^2 = M^2 + M'^2 - 2MM'\omega$, with M, M' the masses of the initial and final hadrons respectively. In addition, $\mathcal{B}_d$ is the branching ratio for the $\tau \to d\nu_\tau$ decay, where d stands for $d = \pi, \rho, \ell\bar{\nu}_\ell$, $\xi_d = E_d/(\gamma m_\tau)$ is the ratio of the energies of the tau-decay massive product (π, ρ or ℓ) and the tau lepton measured in the $\tau\bar{\nu}_\tau$ center of mass frame (CM), with $\gamma = (q^2 + m_\tau^2)/(2m_\tau\sqrt{q^2})$, and the related variable $\beta = (1 - 1/\gamma^2)^{1/2} = (q^2 - m_\tau^2)/(q^2 + m_\tau^2)$, defining the boost from the tau-rest frame to the CM one. θ_d is the angle made by the tree-momenta of the final hadron and the tau-decay massive product in the CM reference system and P_2 is the Legendre polynomial of order two. Besides, $d\Gamma_{\rm SL}/d\omega$ is the unpolarized differential semileptonic $H_b \to H_c\tau\bar{\nu}_\tau$ decay width that can be written as

$$\frac{d\Gamma_{\rm SL}}{d\omega} = \frac{G_F^2 |V_{cb}|^2 M'^3 M^2}{24\pi^3}\sqrt{\omega^2-1}\Big(1 - \frac{m_\tau^2}{q^2}\Big)^2 n_0(\omega), \tag{3}$$

where $n_0(\omega) = 3a_0(\omega) + a_2(\omega)$, with $a_{0,2}(\omega)$ given in Refs. [50, 65], contains all the dynamical effects including any possible NP contribution to the $b \to c$ transition. Finally, the $F_{012}^d(\omega,\xi_d)$ two dimensional functions can be written as[2]

$$\begin{aligned}
F_0^d(\omega,\xi_d) &= C_n^d(\omega,\xi_d) + C_{P_L}^d(\omega,\xi_d)\,\langle P_L^{\rm CM}\rangle(\omega),\\
F_1^d(\omega,\xi_d) &= C_{A_{FB}}^d(\omega,\xi_d) A_{FB}(\omega) + C_{Z_L}^d(\omega,\xi_d) Z_L(\omega) + C_{P_T}^d(\omega,\xi_d)\,\langle P_T^{\rm CM}\rangle(\omega),\\
F_2^d(\omega,\xi_d) &= C_{A_Q}^d(\omega,\xi_d) A_Q(\omega) + C_{Z_Q}^d(\omega,\xi_d) Z_Q(\omega) + C_{Z_\perp}^d(\omega,\xi_d) Z_\perp(\omega).
\end{aligned} \tag{4}$$

where the $C_a^d(\omega,\xi_d)$ are kinematical coefficients that depend on the tau-decay mode. Their analytical expressions can be found, for the $\pi\nu_\tau, \rho\nu_\tau$ and $\ell\bar{\nu}_\ell\nu_\tau$ cases, in Appendix G of Ref. [69]. In the leptonic mode we have kept effects due to the finite mass of the outgoing muon/electron, although making $m_\ell = 0$ in those expressions should be a very good approximation, since both $m_e, /m_\tau$ and m_μ/m_τ are much smaller than one. The rest of the quantities in Eq. (4) are the tau-spin ($\langle P_{L,T}^{\rm CM}\rangle(\omega)$), tau-angular ($A_{FB,Q}(\omega)$) and tau-angular-spin ($Z_{L,Q,\perp}(\omega)$) asymmetries of the $H_b \to H_c\tau\bar{\nu}_\tau$ decay. Actually, these asymmetries and $d\Gamma_{\rm SL}/d\omega$ provide the maximal information that can be extracted from the study of polarized $H_b \to H_c\tau\bar{\nu}_\tau$ transitions, without considering CP non-conserving contributions [49, 69][3] (see Eq. (3.46) of the latter of these two references and the related discussion).

In Ref. [69], we numerically analyzed the role that each of the observables, $d\Gamma_{\rm SL}/d\omega$, $\langle P_{L,T}^{\rm CM}\rangle(\omega)$, $A_{FB,Q}(\omega)$ and $Z_{L,Q,\perp}(\omega)$ could play to establish the existence of NP beyond the SM in $\Lambda_b \to \Lambda_c\tau\bar{\nu}_\tau$ semileptonic decays. In fact in that work, we obtained their general expressions, valid for any

[2] This angular decomposition was firstly introduced in [68] in the context of the $\tau-$hadronic decay modes in $\bar{B} \to D^{(*)}$ reactions.

[3] As discussed in these two references (see also [68]), the azimuthal angular (ϕ_d) distribution of the tau decay charged product turn out to be sensitive to possible CP odd effects, which are produced by the existence of relative phases between some of the Wilson coefficients in the NP Hamiltonian of Eq. (5). However, the measurement of the angle ϕ_d (see Fig. 1) would require the full reconstruction of the tau three momentum. For $\bar{B} \to D^*$ ($\Lambda_b \to \Lambda_c$), some CP-odd observables (triple product asymmetries), defined using angular distributions involving the kinematics of the products of the D^* (Λ_c) decay, have also been presented [33, 34, 36, 48] ([61, 63]).

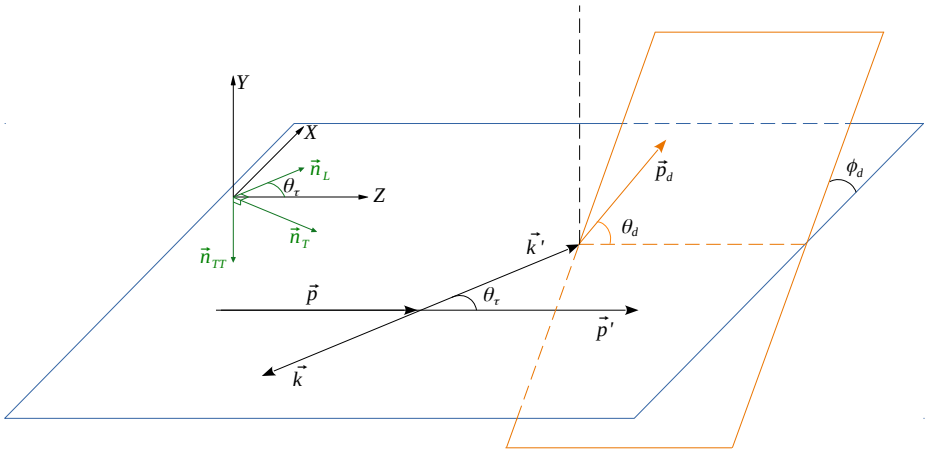

FIG. 1. Kinematics in the $\tau\bar{\nu}_\tau$ CM reference system associated with Eq. (2), and used in Ref. [69]. The initial and final hadron three-momenta are $\vec{p}$ and $\vec{p}'$, respectively, with $\vec{q} = \vec{p} - \vec{p}' = \vec{0}$, while $\vec{k}'$ and $\vec{k}$ are those of the intermediate τ and outgoing $\bar{\nu}_\tau$ emerging from the primary CC transition ($\vec{q} = \vec{k} + \vec{k}' = \vec{0}$). In addition, $\vec{p}_d$ is the momentum of the tau-decay massive product (μ, π or ρ). We also show the unit vectors ($\vec{n}_L, \vec{n}_T$ and $\vec{n}_{TT}$) which define the three independent projections of the $\tau-$polarization vector (see Ref. [49]).

$H_b \to H_c \tau \bar{\nu}_\tau$ decay, when considering an extension of the SM comprising the full set of dimension-6 semileptonic $b \to c$ operators with left- and right-handed neutrinos. The effective low-energy Hamiltonian for that case is given by [45]

$$H_{\rm eff} = \frac{4G_F V_{cb}}{\sqrt{2}} \left[(1 + C_{LL}^V)\mathcal{O}_{LL}^V + C_{RL}^V \mathcal{O}_{RL}^V + C_{LL}^S \mathcal{O}_{LL}^S + C_{RL}^S \mathcal{O}_{RL}^S + C_{LL}^T \mathcal{O}_{LL}^T \right.$$
$$\left. + C_{LR}^V \mathcal{O}_{LR}^V + C_{RR}^V \mathcal{O}_{RR}^V + C_{LR}^S \mathcal{O}_{LR}^S + C_{RR}^S \mathcal{O}_{RR}^S + C_{RR}^T \mathcal{O}_{RR}^T \right] + h.c., \tag{5}$$

with left-handed neutrino fermionic operators given by

$$\mathcal{O}_{(L,R)L}^V = (\bar{c}\gamma^\mu b_{L,R})(\bar{\ell}\gamma_\mu \nu_{\ell L}),\ \mathcal{O}_{(L,R)L}^S = (\bar{c}\, b_{L,R})(\bar{\ell}\, \nu_{\ell L}),\ \mathcal{O}_{LL}^T = (\bar{c}\,\sigma^{\mu\nu} b_L)(\bar{\ell}\sigma_{\mu\nu}\nu_{\ell L}) \tag{6}$$

and the right-handed neutrino ones

$$\mathcal{O}_{(L,R)R}^V = (\bar{c}\gamma^\mu b_{L,R})(\bar{\ell}\gamma_\mu \nu_{\ell R}),\ \mathcal{O}_{(L,R)R}^S = (\bar{c}\, b_{L,R})(\bar{\ell}\, \nu_{\ell R}),\ \mathcal{O}_{RR}^T = (\bar{c}\,\sigma^{\mu\nu} b_R)(\bar{\ell}\sigma_{\mu\nu}\nu_{\ell R}), \tag{7}$$

and where $\psi_{R,L} = (1 \pm \gamma_5)\psi/2$, $G_F = 1.166 \times 10^{-5}$ GeV^{-2} and V_{cb} is the corresponding Cabibbo-Kobayashi-Maskawa matrix element.

The asymmetries introduced in Eq. (4) depend on the pure hadronic structure functions and ten (complex) Wilson coefficients C_{AB}^X ($X = S, V, T$ and $A, B = L, R$), which parameterize the possible deviations from the SM. The former depend on the form factors that parameterize the hadronic current and we have obtained them for $1/2^+ \to 1/2^+$ [65] and $0^- \to 0^-, 1^-$ [50] decays.

The $d^3\Gamma_d/(d\omega d\xi_d d\cos\theta_d)$ distribution, together with the combined analysis of its $(\xi_d, \cos\theta_d)$ dependence, gives access to all the above asymmetries as functions of ω. The feasibility of such studies can be severely limited, however, by the statistical precision in the measurement of the triple differential decay width. Statistics can be increased by integrating in the $\cos\theta_d$ or/and ξ_d

variables, although in this case not all observables can be extracted. Thus, it is well known [70] that the distribution obtained after accumulating in the polar angle,

$$\frac{d^2\Gamma_d}{d\omega d\xi_d} = 2\mathcal{B}_d \frac{d\Gamma_{\rm SL}}{d\omega}\Big\{C_n^d(\omega,\xi_d) + C_{P_L}^d(\omega,\xi_d)\,\langle P_L^{\rm CM}\rangle(\omega)\Big\}, \tag{8}$$

allows to determine $d\Gamma_{\rm SL}/d\omega$ and the CM τ longitudinal polarization $[\langle P_L^{\rm CM}\rangle(\omega)]$ since the, transition dependent, $C_n^d(\omega,\xi_d)$ and $C_{P_L}^d(\omega,\xi_d)$ coefficients are known kinematical factors [69] (see also [67, 70]). The averaged CM tau longitudinal polarization asymmetry,

$$P_\tau = -\frac{1}{\Gamma_{\rm SL}}\int d\omega \frac{d\Gamma_{\rm SL}}{d\omega}\langle P_L^{\rm CM}\rangle(\omega) \tag{9}$$

measured by Belle [5] for the $\bar{B}\to D^*\tau\bar{\nu}_\tau$ decay, immediately follows.

In Refs. [49, 69] we presented results for $\langle P_L^{\rm CM}\rangle(\omega)$ in the $\Lambda_b\to\Lambda_c\tau\bar{\nu}_\tau$ and $\bar{B}\to D^{(*)}\tau\bar{\nu}_\tau$ decays evaluated within the SM and different NP extensions[4]. We also provided similar comparisons for $d\Gamma_{\rm SL}/d\omega$ in the $\Lambda_b\to\Lambda_c$ and $\bar{B}\to D^{(*)}$ and $\bar{B}_c\to J/\psi,\eta_c$ reactions in Refs. [64, 65] and [50], respectively.

In this work, we take advantage of the analytical results derived in [69], and we study, in secs. II, III and IV, respectively, the alternative distributions $d^2\Gamma_d/(d\omega d\cos\theta_d)$, $d\Gamma_d/d\cos\theta_d$ and $d\Gamma_d/dE_d$, which could also be measured in the near future with certain precision. We pay attention to the deviations with respect to the predictions of the SM for these new observables, considering NP operators constructed using both right- and left-handed neutrino fields, within the effective theory approach established by Eqs. (5)–(7). We will present results for the $\Lambda_b\to\Lambda_c\tau\,(\mu\bar{\nu}_\mu\nu_\tau,\pi\nu_\tau,\rho\nu_\tau)\bar{\nu}_\tau$ (main text) and the $\bar{B}\to D^{(*)}\tau\,(\mu\bar{\nu}_\mu\nu_\tau,\pi\nu_\tau,\rho\nu_\tau)\bar{\nu}_\tau$ sequential decays (Appendix B), obtained within different beyond the SM scenarios, and we discuss their use to extract some of the tau asymmetries introduced in Eq. (4). Details on the used form-factors and references to the original works where they were calculated can be found in [49, 69].

II. THE $d^2\Gamma/(d\omega d\cos\theta_d)$ DISTRIBUTION

The limits[5] on the ξ_d variable are tau-decay mode dependent and thus, one has [69]

$$\begin{aligned}
\tau\to\mu\bar{\nu}_\mu\nu_\tau &\Rightarrow y/\gamma \le \xi_d \le \xi_2,\\
\tau\to(\pi,\rho)\nu_\tau &\Rightarrow \frac{1-\beta}{2}+\frac{1+\beta}{2}y^2 = \xi_1 \le \xi_d \le \xi_2 = \frac{1+\beta}{2}+\frac{1-\beta}{2}y^2,
\end{aligned} \tag{10}$$

with $y = m_d/m_\tau$ and m_d the mass of the tau-decay massive product (π, ρ or μ). After integration one obtains the double differential decay width

$$\frac{d^2\Gamma_d}{d\omega d\cos\theta_d} = \mathcal{B}_d\frac{d\Gamma_{\rm SL}}{d\omega}\Big[\widetilde{F}_0^d(\omega)+\widetilde{F}_1^d(\omega)\cos\theta_d+\widetilde{F}_2^d(\omega)P_2(\cos\theta_d)\Big], \tag{11}$$

where the new angular expansion coefficients $\widetilde{F}_{0,1,2}^d(\omega)$ correspond to

$$\widetilde{F}_{0,1,2}^{d=\pi,\rho}(\omega) = \int_{\xi_1}^{\xi_2} F_{0,1,2}^d(\omega,\xi_d)\,d\xi_d, \qquad \widetilde{F}_{0,1,2}^{d=\ell\bar{\nu}_\ell}(\omega) = \int_{y/\gamma}^{\xi_2} F_{0,1,2}^{d=\ell\bar{\nu}_\ell}(\omega,\xi_d)\,d\xi_d \tag{12}$$

[4] We would like to highlight that in Ref. [69] and for the baryon reaction, we showed also results for the CP-violating observable P_{TT}, calculated using the R_2 leptoquark model of Ref. [43]. This is the τ-polarization component along an axis perpendicular to the hadron-tau plane (see Fig. 1). The contribution of P_{TT} to the differential $H_b\to H_c\tau\,(\mu\bar{\nu}_\mu\nu_\tau,\pi\nu_\tau,\rho\nu_\tau)\bar{\nu}_\tau$ distribution disappears when the azimuthal angle ϕ_d is integrated out.

[5] In the case of the lepton mode, the lowest one could be either y/γ or ξ_1 depending on whether q^2 is smaller than or greater than m_τ^4/m_d^2, respectively. Obviously, given the range of q^2 values which can be accessed in the semileptonic $H_b\to H_c$ parent decays and the masses of the charged leptons, we are always in the first of the two scenarios.

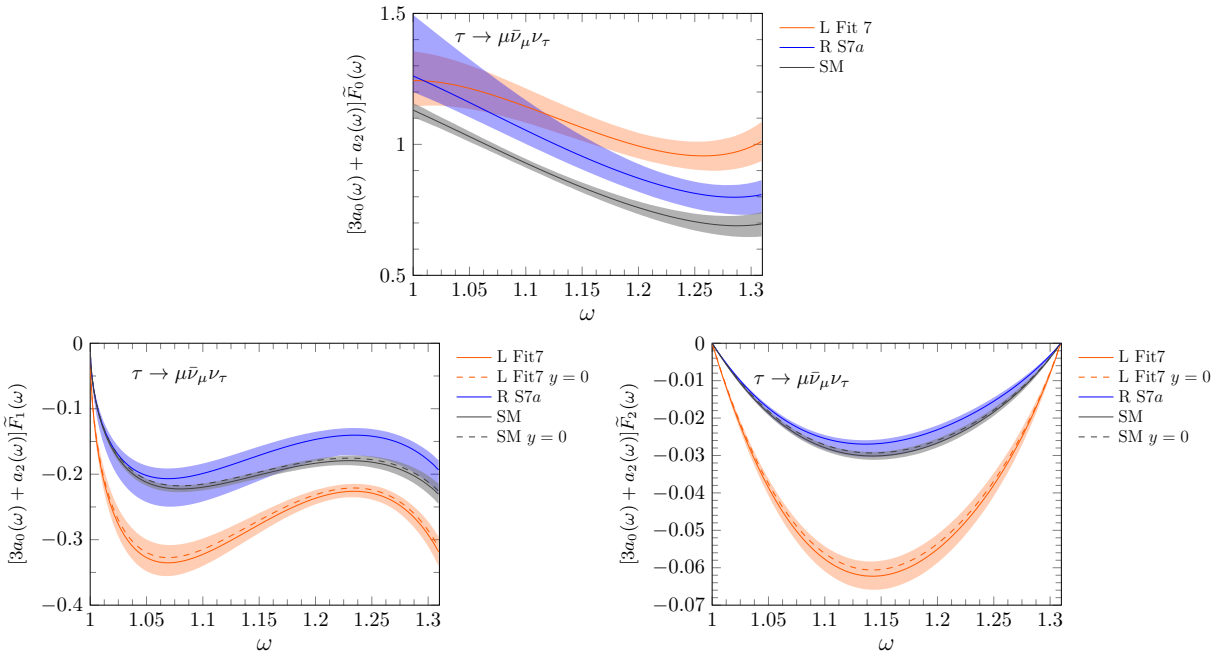

FIG. 2. Results for the functions $[3a_0(\omega)+a_2(\omega)]\widetilde{F}^{\mu\bar{\nu}_\mu}_{0,1,2}(\omega)$ evaluated for the $\Lambda_b \to \Lambda_c\tau(\mu\bar{\nu}_\mu\nu_\tau)\bar{\nu}_\tau$ decay, keeping the muon mass finite, and obtained from the SM and the NP models corresponding to Fit 7 of Ref [42] and Fit 7a of Ref [45]. Error bands account for uncertainties induced by both form-factors and fitted Wilson coefficients (added in quadrature). In the SM and Fit 7 cases, we also display the results obtained neglecting the muon mass, as in Eqs. (15)-(17).

and they can be extracted from the angular analysis of the statistically enhanced $d^2\Gamma/(d\omega d\cos\theta_d)$ distribution. The overall normalization is recovered since $\widetilde{F}^d_0(\omega) = 1/2$ for all tau-decay modes, and a further integration in the polar angle θ_d provides $d\Gamma_d/d\omega = \mathcal{B}_d\, d\Gamma_{\rm SL}/d\omega$, which in this way can be experimentally obtained from the tau decay-chain reaction.

In what follows, we will focus on the non-trivial $\widetilde{F}^d_1(\omega)$ and $\widetilde{F}^d_2(\omega)$ functions, which read

$$\widetilde{F}^d_1(\omega) = C^d_{A_{FB}}(\omega)\, A_{FB}(\omega) + C^d_{Z_L}(\omega)\, Z_L(\omega) + C^d_{P_T}(\omega)\, \langle P^{\rm CM}_T\rangle(\omega), \tag{13}$$

$$\widetilde{F}^d_2(\omega) = C^d_{A_Q}(\omega)\, A_Q(\omega) + C^d_{Z_Q}(\omega)\, Z_Q(\omega) + C^d_{Z_\perp}(\omega)\, Z_\perp(\omega). \tag{14}$$

While the ξ_d integration which gives rise to $\widetilde{F}^d_0(\omega)$ loses information on $\langle P^{\rm CM}_L\rangle(\omega)$, the statistically enhanced observables $\widetilde{F}^{\mu\bar{\nu}_\mu}_{1,2}(\omega)$ retain all the information on the other six asymmetries.

A. Tau-decay lepton mode

We start with the $\tau \to \mu\bar{\nu}_\mu\nu_\tau$ channel, since a measurement of the ratio of branching fractions $\mathcal{B}(\Lambda_b \to \Lambda_c\tau(\mu\nu_\tau\bar{\nu}_\mu)\bar{\nu}_\tau)/\mathcal{B}(\Lambda_b \to \Lambda_c\mu\bar{\nu}_\mu)$ is in progress at the LHCb experiment. Moreover, as argued in the introduction, it would be very important to confront the recent LHCb measurement of $\mathcal{R}_{\Lambda_c}$, reconstructed using the three-prong hadronic τ decay, with results obtained when the tau lepton is identified from its leptonic decay into a muon. In the $y = m_\mu/m_\tau = 0$ limit, which is a very good approximation ($\mathcal{O}(y^2) \sim 1\%$) in this case, and it is much better for the electron

tau-decay mode, we find that the coefficient-functions, $C_a^{\mu\bar{\nu}_\mu}(\omega)$, are given by

$$C_{A_{FB}}^{\mu\bar{\nu}_\mu}(\omega)\Big|_{y=0} = \frac{3\pi\gamma\beta}{2} C_{P_T}^{\mu\bar{\nu}_\mu}(\omega)\Big|_{y=0} = \frac{1}{\beta^2}\Big[\beta - \frac{\operatorname{artanh}\beta}{\gamma^2}\Big], \tag{15}$$

$$C_{A_Q}^{\mu\bar{\nu}_\mu}(\omega)\Big|_{y=0} = -2\beta\gamma C_{Z_\perp}^{\mu\bar{\nu}_\mu}(\omega)\Big|_{y=0} = -\frac{1}{\beta^3}\Big[2\beta^3 - 3\beta + 3\frac{\operatorname{artanh}\beta}{\gamma^2}\Big], \tag{16}$$

$$C_{Z_L}^{\mu\bar{\nu}_\mu}(\omega)\Big|_{y=0} = \frac{1}{3\gamma^2\beta^3}\Big[\beta - \operatorname{artanh}\beta\Big], \quad C_{Z_Q}^{\mu\bar{\nu}_\mu}(\omega)\Big|_{y=0} = \frac{1}{2\gamma^2\beta^4}\Big[3\beta - \big(3-\beta^2\big)\operatorname{artanh}\beta\Big], \tag{17}$$

with $\operatorname{artanh}\beta = \ln\sqrt{\big(1+\beta\big)/\big(1-\beta\big)}$.

Here, we will present results for $\widetilde{F}_{0,1,2}^{\mu\bar{\nu}_\mu}(\omega)$ multiplied by the factor $n_0(\omega)$. For $\widetilde{F}_0^{\mu\bar{\nu}_\mu}(\omega)$ this amounts to represent $n_0(\omega)/2$ and, since this is the same for all tau-decay modes, it will only be shown for the muon tau-decay mode. As mentioned, the $n_0(\omega)$ function, introduced in Eq. (3), contains all the dynamical effects included in the $d\Gamma_{\rm SL}/d\omega$ differential semileptonic decay width, which appears as an overall normalization of the $d^2\Gamma/(d\omega d\cos\theta_d)$ distribution. By showing $\widetilde{F}_{0,1,2}^{\mu\bar{\nu}_\mu}(\omega)$ times $n_0(\omega)$, we access to all the effects of possible NP beyond the SM on the tau production[6].

The $n_0(\omega)\widetilde{F}_{0,1,2}^{\mu\bar{\nu}_\mu}(\omega)$ functions, for the baryon $\Lambda_b \to \Lambda_c\tau(\mu\bar{\nu}_\mu\nu_\tau)\bar{\nu}_\tau$ reaction, are displayed in Fig. 2. They have been evaluated within the SM and the beyond the SM scenarios of Fit 7 (7a) of Ref [42] ([45]), which only includes left- (right-)handed neutrino NP operators. These two NP scenarios have been adjusted to reproduce the anomalies observed in the LFU $\mathcal{R}_D$ and $\mathcal{R}_{D^*}$ ratios in $\bar{B}-$meson decays. However, in all cases, we see the results from Fit 7 of Ref [42] can be distinguished clearly from SM and Fit 7a model (R S7a in the plots) ones. The results for the Fit 7a model are closer to the SM and in the case of the $\widetilde{F}_{1,2}^{\mu\bar{\nu}_\mu}(\omega)$ functions the uncertainty bands overlap in the whole ω interval. This is a reflection of what is obtained for the tau-asymmetries themselves, as can be seen in Fig.2 of Ref. [69].

It is also very instructive to compare the full results for $n_0(\omega)\widetilde{F}_{1,2}^{\mu\bar{\nu}_\mu}(\omega)$ with those evaluated setting $A_{FB}(\omega)$ and $A_Q(\omega)$ to zero. This comparison is presented in Fig. 3. What can be inferred from this comparison is that the contribution of the spin ($\langle P_T^{\rm CM}\rangle(\omega)$) and angular-spin ($Z_{L,Q,\perp}(\omega)$) asymmetry terms are sizable and dominant in most of the ω interval. This is clearly the case in the vicinity of the end-point of the distributions, $q^2 = m_\tau^2$ ($\beta = 0$). In fact, using Eqs. (15)-(17), we find in the $y \to 0$ limit

$$\begin{aligned}\widetilde{F}_1^{\mu\bar{\nu}_\mu}(\omega) \sim{}& \frac{1}{9\pi}\Big[4\langle P_T^{\rm CM}\rangle(\omega_{\rm max}) - \pi Z_L(\omega_{\rm max})\Big] + \frac{\beta}{9}\Big[6A_{FB}(\omega_{\rm max}) \\ &- \frac{m_\tau^2}{\pi MM'}\big[4\langle P_T^{\rm CM}\rangle'(\omega_{\rm max}) - \pi Z_L'(\omega_{\rm max})\big]\Big] + \mathcal{O}(\beta^2),\end{aligned} \tag{18}$$

$$\begin{aligned}\widetilde{F}_2^{\mu\bar{\nu}_\mu}(\omega) \sim{}& -\frac{\beta}{15}\Big[3Z_\perp(\omega_{\rm max}) + 2Z_Q(\omega_{\rm max})\Big] + \frac{\beta^2}{15}\Big[6A_Q(\omega_{\rm max}) \\ &+ \frac{m_\tau^2}{MM'}\big[3Z_\perp'(\omega_{\rm max}) + 2Z_Q'(\omega_{\rm max})\big]\Big] + \mathcal{O}(\beta^3),\end{aligned} \tag{19}$$

with $\omega_{\rm max} = \omega(q^2 = m_\tau^2) = (M^2 + M'^2 - m_\tau^2)/(2MM')$, which show that the contributions of the tau-angular asymmetries A_{FB} and A_Q are suppressed by a factor β with respect to those proportional to $\langle P_T^{\rm CM}\rangle$ and $Z_{L,Q,\perp}$.

Thus, these two $\widetilde{F}_{1,2}^{\mu\bar{\nu}_\mu}(\omega)$ observables, which have an increased statistics over $F_{1,2}^{\mu\bar{\nu}_\mu}(\omega,\xi_d)$, could be ideal to measure tau-spin related asymmetries other than the commonly reported $\langle P_L^{\rm CM}\rangle(\omega)$, extracted from the $d^2\Gamma_d/(d\omega dE_d)$ distribution.

[6] However, we should note that NP contributions to the τ decay are not considered in this work

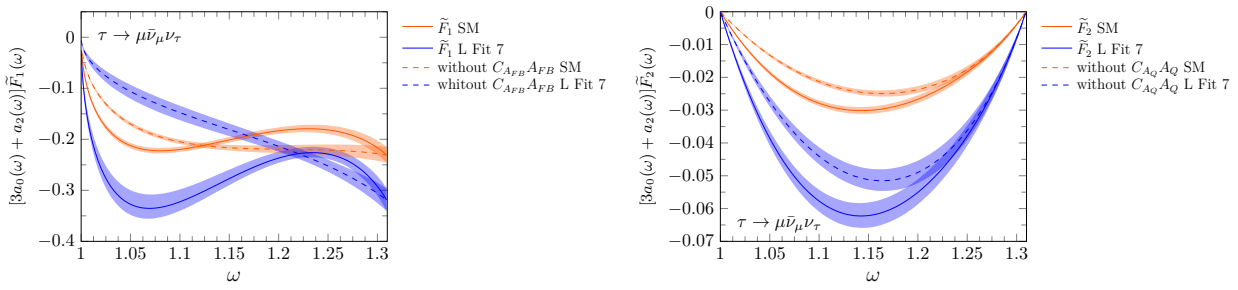

FIG. 3. Comparison of the full results (solid lines) for $[3a_0(\omega)+a_2(\omega)]\widetilde{F}_{1,2}^{\mu\bar{\nu}_\mu}(\omega)$ with those obtained setting $A_{FB}(\omega)$ and $A_Q(\omega)$ to zero (dashed lines). The muon mass is kept finite. The results have been obtained for the $\Lambda_b \to \Lambda_c\tau(\mu\bar{\nu}_\mu\nu_\tau)\bar{\nu}_\tau$ sequential decay, within the SM and the NP model corresponding to Fit 7 of Ref [42].

B. Tau-decay hadron modes

The behavior seen in Fig. 3 of the previous section for the muon is enhanced in the pion decay mode. After performing the integration over the variable ξ_d, we have that, neglecting y^2 (m_μ^2/m_τ^2 and m_π^2/m_τ^2) corrections, the coefficients multiplying the two angular asymmetries $A_{FB,Q}(\omega)$ are the same as in the leptonic mode, while for the rest of the spin and angular-spin asymmetries there is an extra factor of -3. This is to say

$$C^{\pi}_{A_{FB},A_Q}(\omega) = C^{\mu\bar{\nu}_\mu}_{A_{FB},A_Q}(\omega) + \mathcal{O}(y^2), \quad C^{\pi}_{P_T,Z_L,Z_Q,Z_\perp}(\omega) = -3\, C^{\mu\bar{\nu}_\mu}_{P_T,Z_L,Z_Q,Z_\perp}(\omega) + \mathcal{O}(y^2) \tag{20}$$

This difference in the spin analyzing power makes the pion tau-decay mode a better candidate for the extraction of information on the spin and angular-spin asymmetries. Exact expressions, without the $y = 0$ approximation, for the π and ρ decay modes are given in Appendix A, although neglecting m_π^2/m_τ^2 contributions is again an excellent approximation for the pion case. For the ρ decay mode, the spin analyzing power is suppressed, with respect to the pion case, by the factor $a_\rho = (m_\tau^2 - 2m_\rho^2)/(m_\tau^2 + 2m_\rho^2) \approx 0.45$ (see Appendix A), although it is still greater than for the lepton decay mode.

Full results, as well as results obtained setting the angular $A_{FB,Q}(\omega)$ asymmetry terms to zero, for the hadron-mode $\widetilde{F}_{1,2}^{\pi,\rho}(\omega)$ functions are shown in Fig. 4 for the $\Lambda_b \to \Lambda_c\tau(\pi\nu_\tau,\, \rho\nu_\tau)\bar{\nu}_\tau$ decays, accounting for all mass term corrections ($y = m_{\pi,\,\rho}/m_\tau \neq 0$). As expected, we see that the hadron modes, in particular the pion one, show a great sensitivity to the spin-angular asymmetries, which could be extracted from $\widetilde{F}_1^{\pi,\rho}(\omega)$ and $\widetilde{F}_2^{\pi,\rho}(\omega)$. These new observables are independent of the $d\Gamma_{\rm SL}/d\omega$ and $\langle P_L^{\rm CM}\rangle(\omega)$ distributions [49, 69], and they will provide new constraints on the physics governing the $\Lambda_b \to \Lambda_c\tau\bar{\nu}_\tau$ parent decay.

The $\Lambda_b \to \Lambda_c\tau(\pi\nu_\tau, \rho\nu_\tau)\bar{\nu}_\tau$ reaction channels have a lower reconstruction efficiency at LHCb than the one driven by the τ-decay lepton mode [29]. However, they might be accessible in the future, or be easier to reconstruct in other machines and/or chains initiated by other parent semileptonic decays. For that reason, in Appendix B we also present results for distributions obtained from the sequential $\bar{B} \to D^{(*)}\tau(\pi\nu_\tau, \rho\nu_\tau)\bar{\nu}_\tau$ decays.

III. THE $d\Gamma/d\cos\theta_d$ DISTRIBUTION

A further integration in ω additionally enhances the statistics. Although it prevents a separate determination of each of the asymmetries, it is still a useful observable in the search for NP beyond

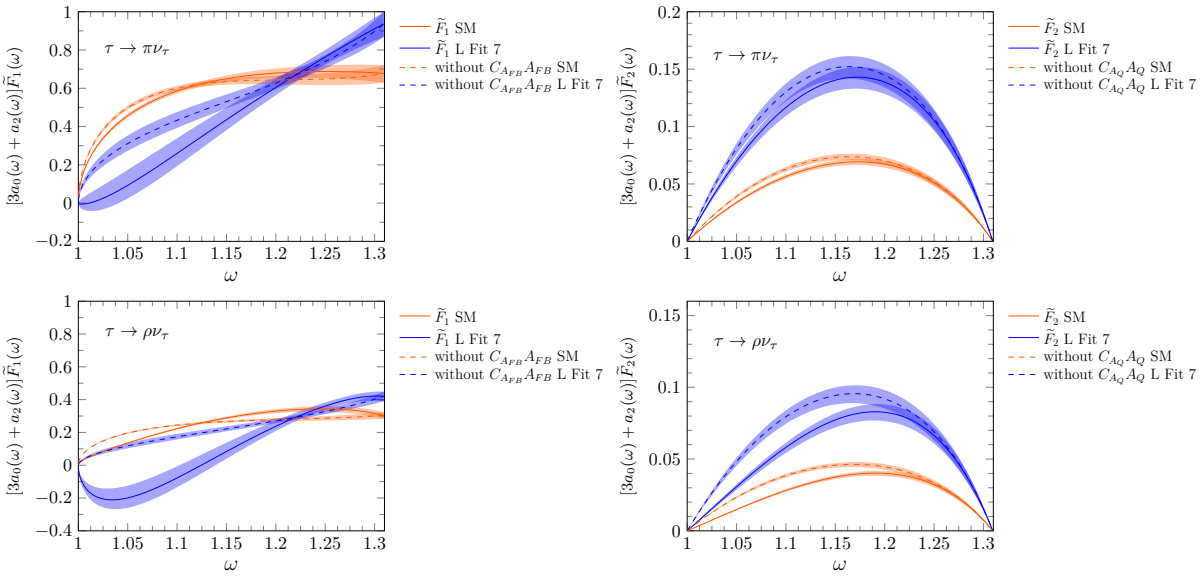

FIG. 4. Same as Fig. 3, but for the $[3a_0(\omega) + a_2(\omega)]\widetilde{F}_{1,2}^{\pi,\rho}(\omega)$ hadron-mode distributions. We use the expressions for the coefficients collected in Appendix A, which were obtained keeping the pion and rho meson masses finite.

the SM. This angular distribution reads

$$\frac{d\Gamma_d}{d\cos\theta_d} = \mathcal{B}_d\Gamma_{\rm SL}\Big[\frac{1}{2} + \widehat{F}_1^d\cos\theta_d + \widehat{F}_2^d\,P_2(\cos\theta_d)\Big], \quad \widehat{F}_{1,2}^d = \frac{1}{\Gamma_{\rm SL}}\int_1^{\omega_{\rm max}}\frac{d\Gamma_{\rm SL}}{d\omega}\widetilde{F}_{1,2}^d(\omega)\,d\omega. \quad (21)$$

and an appropriate angular analysis of $d\Gamma/d\cos\theta_d$ should allow to determine the total semileptonic width $\Gamma_{\rm SL}$ and the moments $\widehat{F}_1^d$ and $\widehat{F}_2^d$.

The full distributions of Eq. (21), normalized by $\mathcal{B}_d\Gamma_{\rm SL}$, for the $\Lambda_b \to \Lambda_c\tau(\mu\bar\nu_\mu\nu_\tau, \pi\nu_\tau, \rho\nu_\tau)\bar\nu_\tau$ chain-decays, evaluated for the SM and different NP models are presented in Fig. 5. The integrated width $\Gamma_{\rm SL}$ and the angular moments $\widehat{F}_1^d$ and $\widehat{F}_2^d$ obtained from, each of the physics scenarios considered in the figure are collected in Tables I and II, respectively. As already mentioned, all NP scenarios have been adjusted to reproduce the anomalies observed in the $\mathcal{R}_D$ and $\mathcal{R}_{D^*}$ ratios in $\bar B-$meson decays, and they all predict values for $\mathcal{R}_{\Lambda_c}$ that are at variance $(2\sigma - 3\sigma)$ with both the SM prediction and the recent LHCb measurement, the latter two being within 1σ. In addition, we also observe differences in $\widehat{F}_1^d$ and $\widehat{F}_2^d$, that are hardly accounted for by errors. This situation is reflected in Fig. 5, where we see that the best discriminating power between the SM and different NP extensions is reached for forward and backward emission in the τ-hadron decay modes, which are more sensitive to $\widehat{F}_1^{\pi,\rho}$ and $\widehat{F}_2^{\pi,\rho}$. In fact, these new observables are shown as excellent tools to discern between different inputs for the semileptonic $\Lambda_b \to \Lambda_c\tau\bar\nu_\tau$ parent reaction.

In Appendix B we collect the corresponding results for the sequential $\bar B \to D^{(*)}\tau(\mu\bar\nu_\mu\nu_\tau, \pi\nu_\tau, \rho\nu_\tau)\bar\nu_\tau$ decays.

IV. THE $d\Gamma/dE_d$ DISTRIBUTION

Finally in this section we study the energy (E_d) distribution of the charged (massive) product from the tau-decay. The idea is to increase the statistics by accumulating events for all allowed ω values and provide only the E_d spectrum. Regardless detector efficiencies considerations, the $d\Gamma/dE_d$ differential decay width could be determined as precisely as $d\Gamma/d\cos\theta_d$ (discussed in

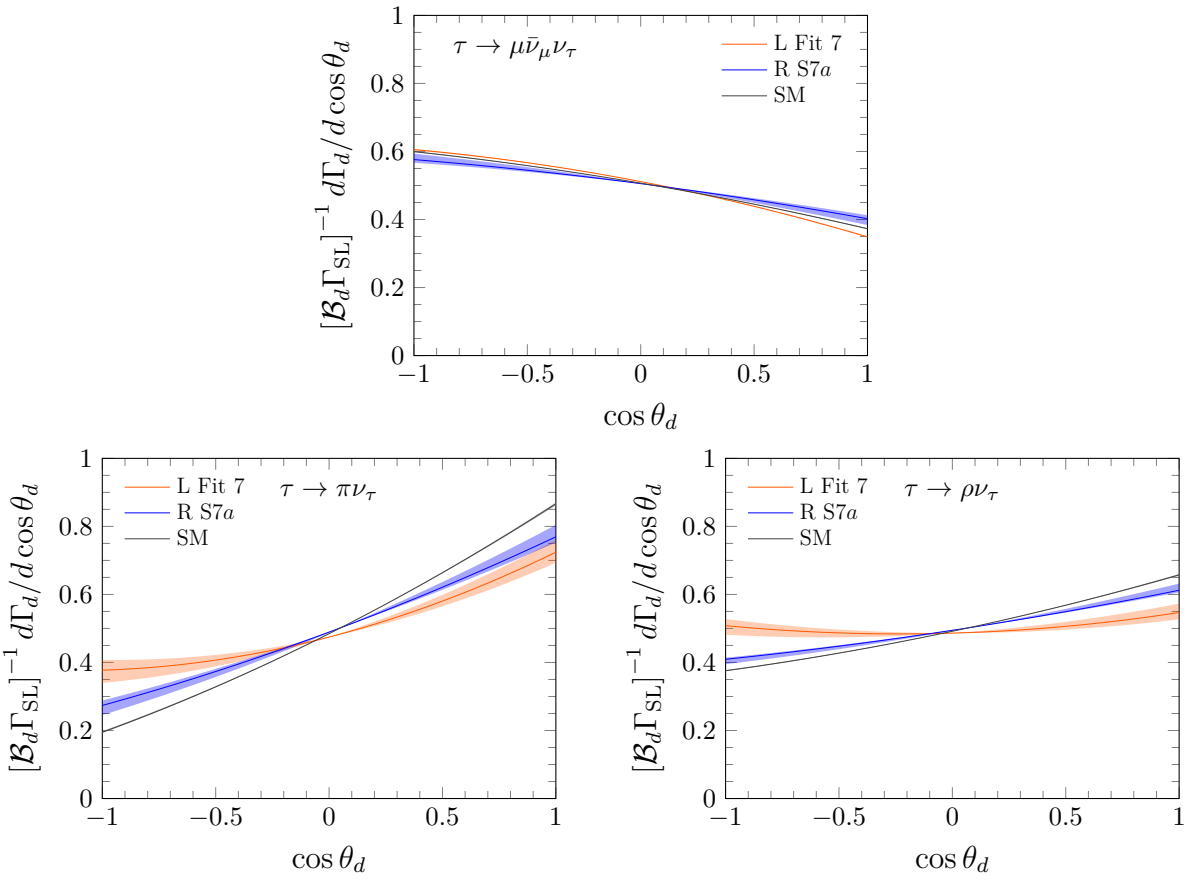

FIG. 5. Angular $d\Gamma/d\cos\theta_d$ distribution for the $\Lambda_b \to \Lambda_c\tau(\mu\bar{\nu}_\mu\nu_\tau,\, \pi\nu_\tau,\, \rho\nu_\tau)\bar{\nu}_\tau$ decays, keeping $y = m_d/m_\tau$ to its finite value, and obtained within the SM and the beyond the SM scenarios of Fit 7 (7a) of Ref [42] ([45]), which only includes left- (right-)handed neutrino NP operators. Error bands account for uncertainties induced by both form-factors and fitted Wilson coefficients (added in quadrature).

Sec. III) or $d\Gamma_{\rm SL}/d\omega$, with the three distributions giving independent information about the dynamics governing the semileptonic $b \to c\tau\bar{\nu}_\tau$ transition [49, 65]. From the $d^2\Gamma_d/(d\omega d\xi_d)$ differential decay width given in Eq. (8) and using $E_d = \gamma m_\tau \xi_d$, we have

$$\frac{d\Gamma_d}{dE_d} = 2\mathcal{B}_d \int_{\omega_{\rm inf}(E_d)}^{\omega_{\rm sup}(E_d)} d\omega \frac{1}{\gamma m_\tau}\frac{d\Gamma_{\rm SL}}{d\omega}\Big\{C_n^d(\omega, E_d) + C_{P_L}^d(\omega, E_d)\,\langle P_L^{\rm CM}\rangle(\omega)\Big\}, \tag{22}$$

The maximum energy, $E_d^{\rm max}$, of the massive product from the tau-decay is

$$E_d^{\rm max} = \frac{(M - M')^2 + m_d^2}{2(M - M')} \tag{23}$$

while the minimum one, $E_d^{\rm min}$, depends on the tau-decay mode and the order relation between $(M - M')$ and m_τ^2/m_d. For the reactions considered in this work, we have $(M - M') \leq m_\tau^2/m_d$ and hence

$$E_d^{\rm min} = m_d, \quad d = \mu\bar{\nu}_\mu, e\bar{\nu}_e \tag{24}$$

$$E_d^{\rm min} = \frac{m_d^2(M - M')^2 + m_\tau^4}{2m_\tau^2(M - M')}, \quad d = \pi, \rho \tag{25}$$

	SM	L Fit 7 [42]	R S7a [45]	LHCb [27]
$\Gamma_{e(\mu)}$	2.15 ± 0.08			
Γ_τ	0.715 ± 0.015	0.89 ± 0.05	0.81 ± 0.06	
$\mathcal{R}_{\Lambda_c}$	0.332 ± 0.007	0.41 ± 0.02	0.38 ± 0.03	$0.242 \pm 0.026 \pm 0.040 \pm 0.059$

TABLE I. Semileptonic decay widths $\Gamma_\tau = \Gamma\left(\Lambda_b \to \Lambda_c \tau \bar{\nu}_\tau\right)$ and $\Gamma_{e(\mu)} = \Gamma\left(\Lambda_b \to \Lambda_c\, e(\mu) \bar{\nu}_{e(\mu)}\right)$ [units of $\left(10 \times |V_{cb}|^2 \text{ps}^{-1}\right)$] and ratios $\mathcal{R}_{\Lambda_c} = \Gamma\left(\Lambda_b \to \Lambda_c \tau \bar{\nu}_\tau\right) / \Gamma\left(\Lambda_b \to \Lambda_c\, e(\mu) \bar{\nu}_{e(\mu)}\right)$ obtained in the SM, the NP model Fit 7 (7a) of Ref [42] ([45]), which only includes left- (right-)handed neutrino NP operators. Errors induced by the uncertainties in the form-factors and Wilson Coefficients are added in quadrature. The recent LHCb [27] measurement of the $\mathcal{R}_{\Lambda_c}$ ratio, with the tau being reconstructed using the $\tau \to \pi^-\pi^+\pi^-(\pi^0)\,\nu_\tau$ decay, is also shown.

	$\widehat{F}_1^{\mu\bar{\nu}_\mu}$	$\widehat{F}_2^{\mu\bar{\nu}_\mu}$	$\widehat{F}_1^{\pi}$	$\widehat{F}_2^{\pi}$	$\widehat{F}_1^{\rho}$	$\widehat{F}_2^{\rho}$
SM	-0.113 ± 0.001	-0.0137 ± 0.0003	0.336 ± 0.003	0.0306 ± 0.0007	0.141 ± 0.002	0.0166 ± 0.0004
L Fit 7	-0.128 ± 0.003	-0.0228 ± 0.0005	0.17 ± 0.03	0.0507 ± 0.0013	$0.019^{+0.025}_{-0.020}$	0.0275 ± 0.0007
R S7a	$-0.087^{+0.010}_{-0.017}$	$-0.0108^{+0.0006}_{-0.0011}$	$0.25^{+0.03}_{-0.02}$	$0.023^{+0.002}_{-0.003}$	$0.101^{+0.017}_{-0.005}$	$0.0108^{+0.0027}_{-0.0008}$

TABLE II. Predictions for the angular moments $\widehat{F}^d_{1,\,2}$ for the $\Lambda_b \to \Lambda_c \tau(\mu\bar{\nu}_\mu\nu_\tau,\, \pi\nu_\tau,\, \rho\nu_\tau)\bar{\nu}_\tau$ decays evaluated in the SM and the same NP scenarios considered in Table I.

while $E_d^{\text{min}} = m_d$ for the hadronic case if $(M - M') \geq m_\tau^2/m_d$. This latter situation occurs for instance in the sequential $\bar{B} \to \pi\tau(\rho\nu_\tau)\bar{\nu}_\tau$ reaction, involving the CC $b \to u\tau\bar{\nu}_\tau$ transition.

To perform the ω integration, first we have to obtain the allowed variation of the ω variable for a given E_d, i.e., to determine $\omega_{\text{inf}}(E_d)$ and $\omega_{\text{sup}}(E_d)$ in Eq. (22). This requires to invert the limits in Eq. (10) and the result depends on the tau-decay channel

1. $\tau \to \mu\bar{\nu}_\mu\nu_\tau$ and $\tau \to e\bar{\nu}_e\nu_\tau$: In this case, m_d is either the muon or the electron mass, and considering $(M - M') \leq m_\tau^2/m_d$, we find $\omega_{\text{inf}}(E_d) = 1$, while

$$\omega_{\text{sup}}(E_d) = \omega_{\text{max}} = \frac{M^2 + M'^2 - m_\tau^2}{2MM'}, \quad E_d \leq \frac{m_\tau^2 + m_d^2}{2m_\tau} \tag{26}$$

$$\omega_{\text{sup}}(E_d) = \frac{M^2 + M'^2 - \left(E_d + \sqrt{E_d^2 - m_d^2}\right)^2}{2MM'}, \quad E_d \geq \frac{m_\tau^2 + m_d^2}{2m_\tau} \tag{27}$$

2. $\tau \to \pi\nu_\tau$ and $\tau \to \rho\nu_\tau$: In this case m_d is either the pion or rho mass, and considering $(M - M') \leq m_\tau^2/m_d$, we also find $\omega_{\text{inf}}(E_d) = 1$, while

$$\omega_{\text{sup}}(E_d) = \frac{M^2 + M'^2 - m_\tau^4\left(E_d - \sqrt{E_d^2 - m_d^2}\right)^2/m_d^4}{2MM'}, \quad E_d \leq \frac{m_\tau^2 + m_d^2}{2m_\tau} \tag{28}$$

$$\omega_{\text{sup}}(E_d) = \frac{M^2 + M'^2 - \left(E_d + \sqrt{E_d^2 - m_d^2}\right)^2}{2MM'}, \quad E_d \geq \frac{m_\tau^2 + m_d^2}{2m_\tau} \tag{29}$$

From the differential distribution of Eq. (22), we define a new dimensionless observable $\widehat{F}_0^d(E_d)$, such that $d\Gamma/dE_d = 2\mathcal{B}_d\Gamma_{\text{SL}}\widehat{F}_0^d(E_d)/m_\tau$, with Γ_{SL} the total $H_b \to H_c\tau\bar{\nu}_\tau$ semileptonic decay width,

and

$$\widehat{F}_0^d(E_d) = \frac{1}{\Gamma_{\rm SL}} \int_1^{\omega_{\rm sup}(E_d)} \frac{1}{\gamma} \frac{d\Gamma_{\rm SL}}{d\omega} \Big\{ C_n^d(\omega, E_d) + C_{P_L}^d(\omega, E_d) \, \langle P_L^{\rm CM} \rangle(\omega) \Big\} \, d\omega, \tag{30}$$

where the corresponding $\omega_{\rm sup}(E_d)$ values can be read out from Eqs. (26)-(29). This energy function is normalized for all tau-decay channels to

$$\frac{1}{m_\tau} \int_{E_d^{\rm min}}^{E_d^{\rm min}} dE_d \widehat{F}_0^d(E_d) = \frac{1}{m_\tau \Gamma_{\rm SL}} \int_{E_d^{\rm min}}^{E_d^{\rm min}} \int_1^{\omega_{\rm sup}(E_d)} \frac{1}{\gamma} \frac{d\Gamma_{\rm SL}}{d\omega} C_n^d(\omega, E_d) \, d\omega dE_d = \frac{1}{2} \tag{31}$$

Although the CM τ longitudinal polarization $\langle P_L^{\rm CM} \rangle(\omega)$ does not contribute to the normalization of $\widehat{F}_0^d(E_d)$, it still affects the energy shape of the observable. This is in contrast to what happens if, instead, one accumulates on the variable ξ_d in the $d^2\Gamma_d/(d\omega d\xi_d)$ distribution of Eq. (8) to obtain $d\Gamma_d/d\omega$. As already mentioned, this ξ_d (or equivalently E_d) integration removes permanently any information about $\langle P_L^{\rm CM} \rangle$.

The results for $\widehat{F}_0^d(E_d)$ in the $\Lambda_b \to \Lambda_c \tau(\mu\bar{\nu}_\mu\nu_\tau,\, \pi\nu_\tau,\, \rho\nu_\tau)\bar{\nu}_\tau$ decays are presented in Fig. 6. We observe small changes between the predictions obtained from the SM and any of the NP models considered in this work, pointing out to a little influence of the $\langle P_L^{\rm CM} \rangle$ contribution in this distribution. Nevertheless, for the hadron modes, we again see that Fit 7 of Ref [42] gives, in some regions, significantly different results from those obtained in the SM and Fit 7a, while the latter agrees with the SM within uncertainty bands.

V. SUMMARY AND CONCLUSIONS

Using the analytical results derived in [69], we have studied the $d^2\Gamma_d/(d\omega d\cos\theta_d)$, $d\Gamma_d/d\cos\theta_d$ and $d\Gamma_d/dE_d$ distributions, which are defined in terms of the visible energy and polar angle of the charged particle from the τ-decay in $b \to c\tau\,(\mu\bar{\nu}_\mu\nu_\tau, \pi\nu_\tau, \rho\nu_\tau)\bar{\nu}_\tau$ reactions and that one expects to be measured at some point in the near future. The first two contain information on the CM transverse tau-spin ($\langle P_T^{\rm CM} \rangle(\omega)$), tau-angular ($A_{FB,Q}(\omega)$) and tau-angular-spin ($Z_{L,Q,\perp}(\omega)$) asymmetries of the $H_b \to H_c\tau\bar{\nu}_\tau$ parent decay. Hence, from the dynamical point of view, these observables are richer than the commonly used one, $d^2\Gamma_d/(d\omega dE_d)$, since the latter gives access only to the CM tau longitudinal polarization $\langle P_L^{\rm CM} \rangle(\omega)$. We have paid attention to the deviations with respect to the predictions of the SM for these new observables, considering NP operators constructed using both left- and right-handed neutrino fields, within an effective theory approach. We have presented results for these distributions in $\Lambda_b \to \Lambda_c\tau\,(\mu\bar{\nu}_\mu\nu_\tau, \pi\nu_\tau, \rho\nu_\tau)\bar{\nu}_\tau$ (main text) and $\bar{B} \to D^{(*)}\tau\,(\mu\bar{\nu}_\mu\nu_\tau, \pi\nu_\tau, \rho\nu_\tau)\bar{\nu}_\tau$ (Appendix B) sequential decays, within different beyond the SM scenarios, and we have discussed their use to disentangle between different NP models. In this respect, we have seen that $d\Gamma_d/d\cos\theta_d$, if measured with sufficiently good statistics, becomes quite useful, especially in the $\tau \to \pi\nu_\tau$ decay mode.

The study carried out in this work acquires a special relevance due to the recent LHCb measurement of the LFU ratio $\mathcal{R}_{\Lambda_c}$ in agreement, within errors, with the SM prediction. The experiment identified the τ using the three-prong hadronic $\tau^- \to \pi^-\pi^+\pi^-(\pi^0)\,\nu_\tau$ decay, and this result for $\mathcal{R}_{\Lambda_c}$, which is in conflict with the phenomenology from the b-meson sector, needs to be confirmed employing other reconstruction channels.

We are aware of the difficulties in measuring the accumulated distributions proposed in this work for the $\Lambda_b \to \Lambda_c\tau(\mu\bar{\nu}_\mu\nu_\tau, \pi\nu_\tau, \rho\nu_\tau)\bar{\nu}_\tau$ decay at LHC [71]. As mentioned in the Introduction, the LHCb collaboration is conducting a study on this reaction using the $\tau \to \mu\bar{\nu}_\mu\nu_\tau$ reconstruction channel. We expect that this would imply the measurement of some of the muon variables and

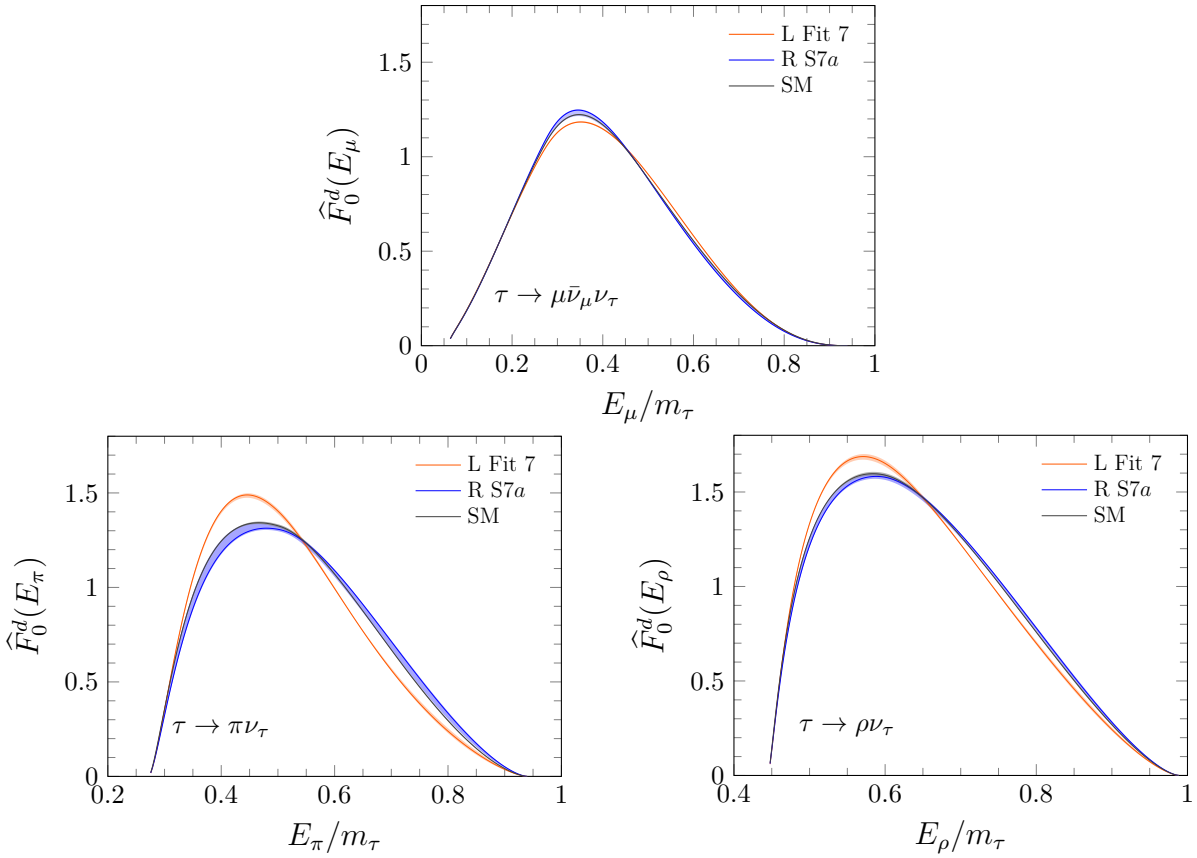

FIG. 6. Predictions for the $\widehat{F}_0^d(E_d)$ energy distribution [Eq. (30)] for the $\Lambda_b \to \Lambda_c\tau(\mu\bar{\nu}_\mu\nu_\tau, \pi\nu_\tau, \rho\nu_\tau)\bar{\nu}_\tau$ decays, keeping $y = m_d/m_\tau$ finite, obtained within the SM and the NP scenarios corresponding to Fit 7 of Ref [42] and Fit 7a of Ref [45].

thus the determination, in the not too distant future and with a certain accuracy, of some or all, of the differential decays widths analyzed in this work. If the presence of NP is confirmed, going beyond the pure measurement of $R(\Lambda_c)$ (and other ratios) is essential to disentangle among different SM extensions. Furthermore, we have also predicted accumulated distributions for the $\bar{B} \to D^{(*)}$ semileptonic reactions, for which, within the context of the plan to increase luminosity at the LHC, the prospects look more favorable [71].

ACKNOWLEDGEMENTS

This research has been supported by the Spanish Ministerio de Ciencia e Innovación (MICINN) and the European Regional Development Fund (ERDF) under contract PID2020-112777GB-I00 and PID2019-105439GB-C22, the EU STRONG-2020 project under the program H2020-INFRAIA-2018-1, grant agreement no. 824093 and by Generalitat Valenciana under contract PROMETEO/2020/023.

Appendix A: Coefficients $C^{\pi,\rho}_{A_{FB,Q}}(\omega)$, $C^{\pi,\rho}_{P_T}(\omega)$ and $C^{\pi,\rho}_{Z_{L,Q,\perp}}(\omega)$ for the $\pi\nu_\tau$ and $\rho\nu_\tau$ τ-decay modes

In this appendix, we give the coefficients which define the $\widetilde{F}^{\pi,\rho}_{12}(\omega)$ distributions in terms of the tau-asymmetries, through Eqs. (13) and (14), for the $\pi\nu_\tau$ and $\rho\nu_\tau$ tau-decay modes keeping

finite $y = m_d/m_\tau$. We use the analytical expressions derived in Ref. [69] for the two dimensional $C^{\pi,\rho}_{A_{FB,Q}}(\omega,\xi_d)$, $C^{\pi,\rho}_{P_T}(\omega,\xi_d)$ and $C^{\pi,\rho}_{Z_{L,Q,\perp}}(\omega,\xi_d)$ functions and integrate over the variable ξ_d. We first discuss the coefficient of the forward-backward asymmetry,

$$C^{\pi,\rho}_{A_{FB}}(\omega) = \begin{cases} \frac{1+y^2}{1-y^2}\frac{1}{\beta^2}\left[\beta - \frac{\operatorname{artanh}\beta}{\gamma^2}\right], & y^2 \le \frac{1-\beta}{1+\beta} = \frac{m_\tau^2}{q^2} \\ \\ \frac{1+y^2}{1-y^2}\frac{1}{\beta^2}\left[\frac{1-y^2}{1+y^2} + \frac{\log y}{\gamma^2}\right], & y^2 \ge \frac{1-\beta}{1+\beta} = \frac{m_\tau^2}{q^2} \end{cases} \tag{A1}$$

For the reactions studied in this work, we always have $y^2 \le m_\tau^2/q^2$ for all available q^2 values and thus, the first of the above possibilities should be taken. The situation is repeated for the rest of the coefficients. For brevity, we only give below the expressions for the $y^2 < m_\tau^2/q^2$ case,

$$C^{\pi,\rho}_{Z_L}(\omega) = -a_{\pi,\rho}\left[\frac{1+4y^2+y^4}{(1-y^2)^2}\frac{1}{\gamma^2\beta^3}\left(\beta - \operatorname{artanh}\beta\right) + \frac{2y^2}{(1-y^2)^2}\right] \tag{A2}$$

$$C^{\pi,\rho}_{P_T}(\omega) = -a_{\pi,\rho}\frac{2}{\pi\gamma\beta}\left[\frac{1+4y^2+y^4}{1-y^4}C^{\pi,\rho}_{A_{FB}}(\omega) - \frac{4y^2}{(1-y^2)^2}\operatorname{artanh}\beta\right] \tag{A3}$$

$$\begin{aligned} C^{\pi,\rho}_{A_Q}(\omega) = {} & \frac{1}{2\beta^2}\left[3 - \beta^2 + 3\frac{1+\left(2+4\gamma^2\right)y^2+y^4}{2\gamma^3\beta y\left(1-y^2\right)}\operatorname{artanh}\left(\frac{2\gamma\beta y}{1-y^2}\right)\right] \\ & -\frac{3}{\gamma^2\beta^3}\frac{1+y^2}{1-y^2}\operatorname{artanh}\left(\frac{1+y^2}{1-y^2}\beta\right) \end{aligned} \tag{A4}$$

$$\begin{aligned} C^{\pi,\rho}_{Z_Q}(\omega) = {} & -3a_{\pi,\rho}\left[\frac{1+y^2}{\beta^3\gamma^2\left(1-y^2\right)}\left(1 + \frac{1}{4\gamma\beta y}\frac{1+\left(10+4\gamma^2\right)y^2+y^4}{1-y^2}\operatorname{artanh}\left(\frac{2\gamma\beta y}{1-y^2}\right)\right)\right. \\ & \left. -\frac{2\gamma^2\left(1+4y^2+y^4\right)+\left(1+y^2\right)^2}{2\gamma^4\beta^4\left(1-y^2\right)^2}\operatorname{artanh}\left(\frac{1+y^2}{1-y^2}\beta\right)\right] \end{aligned} \tag{A5}$$

$$\begin{aligned} C^{\pi,\rho}_{Z_\perp}(\omega) = {} & \frac{3a_{\pi,\rho}}{2\beta^4\gamma}\frac{1}{\left(1-y^2\right)^2}\left[\left(2\beta-\beta^3\right)\left(1-y^4\right) - \frac{3\left(1+y^2\right)^2+4\gamma^2y^2}{\gamma^2}\operatorname{artanh}\left(\frac{1+y^2}{1-y^2}\beta\right)\right. \\ & \left. +\frac{1+y^2}{2y}\frac{\left(1+y^2\right)^2+12\gamma^2y^2}{\gamma^3}\operatorname{artanh}\left(\frac{2\gamma\beta y}{1-y^2}\right)\right] \end{aligned} \tag{A6}$$

with $a_\pi = 1$ and $a_\rho = (m_\tau^2 - 2m_\rho^2)/(m_\tau^2 + 2m_\rho^2)$. Note that all the arguments of the artanh-functions are smaller than one, since the above expressions are only valid for $y^2 < (1-\beta)/(1+\beta)$.

Appendix B: Results for the $\bar{B} \to D^{(*)}\tau(\mu\bar{\nu}_\mu\nu_\tau, \pi\nu_\tau, \rho\nu_\tau)\bar{\nu}_\tau$ sequential decays

In this appendix we collect some results for the $\bar{B} \to D^{(*)}\tau(\mu\bar{\nu}_\mu\nu_\tau\pi\nu_\tau, \rho\nu_\tau)\bar{\nu}_\tau$ sequential decays. We start by showing, in Figs. 7 and 8, the $\widetilde{F}^d_{0,1,2}(\omega)$ functions evaluated within the SM and the NP models corresponding to Fit 7 of Ref [42] and Fit 7a of Ref [45], which only includes left-(right-)handed neutrino NP operators, respectively. Similarly to the $\Lambda_b \to \Lambda_c$ decay, the results for Fit 7 are very different from those obtained with Fit 7a and the SM, the latter two agreeing within uncertainties.

In Figs. 9 and 10, we present now the $d\Gamma/d\cos\theta_d$ distributions predicted within the SM and the beyond the SM scenarios of Fits 7 and 7a of Refs. [42] and [45], respectively. The best discriminating power is reached for forward and backward emission in the τ-hadron decay modes for the $\bar{B} \to D$ decay.

		SM	L Fit 7 [42]	R S7a [45]	HFLAV [10]
$\bar{B} \to D$	$\Gamma_{e(\mu)}$	0.87 ± 0.03			
	Γ_τ	0.262 ± 0.005	0.34 ± 0.04	$0.292^{+0.060}_{-0.014}$	
	$\mathcal{R}_D$	$0.300^{+0.005}_{-0.004}$	$0.388^{+0.044}_{-0.045}$	$0.334^{+0.070}_{-0.015}$	$0.340 \pm 0.027 \pm 0.013$
$\bar{B} \to D^*$	$\Gamma_{e(\mu)}$	$2.01^{+0.07}_{-0.08}$			
	Γ_τ	$0.512^{+0.013}_{-0.014}$	0.61 ± 0.03	0.59 ± 0.03	
	$\mathcal{R}_{D^*}$	0.255 ± 0.003	0.306 ± 0.013	$0.292^{+0.014}_{-0.015}$	$0.295 \pm 0.011 \pm 0.008$

TABLE III. Semileptonic decay widths $\Gamma_\tau = \Gamma\left(\bar{B} \to D^{(*)}\tau\bar{\nu}_\tau\right)$ and $\Gamma_{e(\mu)} = \Gamma\left(\bar{B} \to D^{(*)}\, e(\mu)\bar{\nu}_{e(\mu)}\right)$ [units of $\left(10 \times |V_{cb}|^2 \mathrm{ps}^{-1}\right)$] and ratios $\mathcal{R}_{D^{(*)}} = \Gamma\left(\bar{B} \to D^{(*)}\tau\bar{\nu}_\tau\right)/\Gamma\left(\bar{B} \to D^{(*)}\, e(\mu)\bar{\nu}_{e(\mu)}\right)$ obtained in the SM, the NP model Fit 7 (7a) of Ref [42] ([45]), which only includes left- (right-)handed neutrino NP operators. Errors induced by the uncertainties in the form-factors and Wilson Coefficients are added in quadrature. The $\mathcal{R}_{D^{(*)}}$ experimental averages compiled by the HFLAV [10] collaboration are also given.

		$\widehat{F}_1^{\mu\bar{\nu}_\mu}$	$\widehat{F}_2^{\mu\bar{\nu}_\mu}$
$\bar{B} \to D$	SM	$-0.06029^{+0.00021}_{-0.00018}$	$-0.03539^{+0.00015}_{-0.00012}$
	L Fit 7	$-0.0306^{+0.0015}_{-0.0012}$	$-0.0777046^{+0.0000051}_{-0.0000004}$
	R S7a	$-0.031^{+0.021}_{-0.042}$	$-0.027^{+0.002}_{-0.003}$
$\bar{B} \to D^*$	SM	$-0.1267^{+0.0012}_{-0.0014}$	-0.0063 ± 0.0003
	L Fit 7	$-0.1695^{+0.0016}_{-0.0017}$	-0.0020 ± 0.0004
	R S7a	$-0.098^{+0.004}_{-0.016}$	$-0.0053^{+0.0007}_{-0.0019}$

TABLE IV. Predictions for the angular moments $\widehat{F}_{1,2}^{\mu\bar{\nu}_\mu}$ for the $\bar{B} \to D^{(*)}\tau(\mu\bar{\nu}_\mu\nu_\tau)\bar{\nu}_\tau$ decay evaluated in the SM and the same NP scenarios considered in Table III.

Finally, in Table III, we collect the values for the integrated $\Gamma_\tau = \Gamma\left(\bar{B} \to D^{(*)}\tau\bar{\nu}_\tau\right)$ and $\Gamma_{e(\mu)} = \Gamma\left[\bar{B} \to D^{(*)}\, e(\mu)\bar{\nu}_{e(\mu)}\right]$ decay widths, as well as the $\mathcal{R}_{D^{(*)}} = \Gamma\left(\bar{B} \to D^{(*)}\tau\bar{\nu}_\tau\right)/\Gamma\left[\bar{B} \to D^{(*)}\, e(\mu)\bar{\nu}_{e(\mu)}\right]$ ratios, obtained in each of the physics scenarios considered in the figures. The corresponding results for the $\widehat{F}_{1,2}^{d}$ angular moments are given in Tables IV and V, for the lepton and hadron modes, respectively.

[1] J. P. Lees *et al.* (BaBar), Phys. Rev. Lett. **109**, 101802 (2012), arXiv:1205.5442 [hep-ex].
[2] J. P. Lees *et al.* (BaBar), Phys. Rev. D **88**, 072012 (2013), arXiv:1303.0571 [hep-ex].
[3] M. Huschle *et al.* (Belle), Phys. Rev. D **92**, 072014 (2015), arXiv:1507.03233 [hep-ex].
[4] Y. Sato *et al.* (Belle), Phys. Rev. D **94**, 072007 (2016), arXiv:1607.07923 [hep-ex].
[5] S. Hirose *et al.* (Belle), Phys. Rev. Lett. **118**, 211801 (2017), arXiv:1612.00529 [hep-ex].
[6] G. Caria *et al.* (Belle), Phys. Rev. Lett. **124**, 161803 (2020), arXiv:1910.05864 [hep-ex].
[7] R. Aaij *et al.* (LHCb), Phys. Rev. Lett. **115**, 111803 (2015), [Erratum: Phys.Rev.Lett. 115, 159901 (2015)], arXiv:1506.08614 [hep-ex].
[8] R. Aaij *et al.* (LHCb), Phys. Rev. Lett. **120**, 171802 (2018), arXiv:1708.08856 [hep-ex].
[9] R. Aaij *et al.* (LHCb), Phys. Rev. D **97**, 072013 (2018), arXiv:1711.02505 [hep-ex].
[10] Y. S. Amhis *et al.* (HFLAV), Eur. Phys. J. C **81**, 226 (2021), arXiv:1909.12524 [hep-ex].
[11] R. Aaij *et al.* (LHCb), Phys. Rev. Lett. **120**, 121801 (2018), arXiv:1711.05623 [hep-ex].
[12] A. Y. Anisimov, I. M. Narodetsky, C. Semay, and B. Silvestre-Brac, Phys. Lett. **B452**, 129 (1999),

		$\widehat{F}_1^\pi$	$\widehat{F}_2^\pi$	$\widehat{F}_1^\rho$	$\widehat{F}_2^\rho$
$\bar{B}\to D$	SM	$0.5427^{+0.0004}_{-0.0005}$	0.0779 ± 0.0003	$0.32388^{+0.00016}_{-0.00022}$	$0.04189^{+0.00017}_{-0.00019}$
	L Fit 7	$0.160^{+0.013}_{-0.016}$	$0.1699^{+0.0007}_{-0.0006}$	$0.089^{+0.008}_{-0.010}$	$0.0910^{+0.0006}_{-0.0005}$
	R S7a	$0.45^{+0.05}_{-0.09}$	$0.053^{+0.011}_{-0.006}$	$0.285^{+0.015}_{-0.055}$	$0.026^{+0.008}_{-0.004}$
$\bar{B}\to D^*$	SM	$0.2732^{+0.0020}_{-0.0016}$	0.0146 ± 0.0007	$0.0889^{+0.0017}_{-0.0019}$	0.0082 ± 0.0004
	L Fit 7	$0.3200^{+0.0005}_{-0.0004}$	0.0053 ± 0.0008	$0.0876^{+0.0010}_{-0.0011}$	0.0032 ± 0.0004
	R S7a	$0.184^{+0.069}_{-0.012}$	$0.0115^{+0.0048}_{-0.0019}$	$0.050^{+0.035}_{-0.005}$	$0.0062^{+0.0028}_{-0.0011}$

TABLE V. Predictions for the angular moments $\widehat{F}^d_{1,\,2}$ for the $\bar{B}\to D^{(*)}\tau(\pi\nu_\tau,\,\rho\nu_\tau)\bar{\nu}_\tau$ decays evaluated in the SM and the same NP scenarios considered in Table III.

arXiv:hep-ph/9812514 [hep-ph].
[13] M. A. Ivanov, J. G. Korner, and P. Santorelli, Phys. Rev. **D73**, 054024 (2006), arXiv:hep-ph/0602050 [hep-ph].
[14] E. Hernández, J. Nieves, and J. Verde-Velasco, Phys. Rev. D **74**, 074008 (2006), arXiv:hep-ph/0607150.
[15] T. Huang and F. Zuo, Eur. Phys. J. **C51**, 833 (2007), arXiv:hep-ph/0702147 [HEP-PH].
[16] W. Wang, Y.-L. Shen, and C.-D. Lu, Phys. Rev. **D79**, 054012 (2009), arXiv:0811.3748 [hep-ph].
[17] W.-F. Wang, Y.-Y. Fan, and Z.-J. Xiao, Chin. Phys. **C37**, 093102 (2013), arXiv:1212.5903 [hep-ph].
[18] R. Watanabe, Phys. Lett. B **776**, 5 (2018), arXiv:1709.08644 [hep-ph].
[19] A. Issadykov and M. A. Ivanov, Phys. Lett. **B783**, 178 (2018), arXiv:1804.00472 [hep-ph].
[20] C.-T. Tran, M. A. Ivanov, J. G. Körner, and P. Santorelli, Phys. Rev. **D97**, 054014 (2018), arXiv:1801.06927 [hep-ph].
[21] X.-Q. Hu, S.-P. Jin, and Z.-J. Xiao, Chin. Phys. **C44**, 023104 (2020), arXiv:1904.07530 [hep-ph].
[22] D. Leljak, B. Melic, and M. Patra, JHEP **05**, 094 (2019), arXiv:1901.08368 [hep-ph].
[23] K. Azizi, Y. Sarac, and H. Sundu, Phys. Rev. **D99**, 113004 (2019), arXiv:1904.08267 [hep-ph].
[24] W. Wang and R. Zhu, Int. J. Mod. Phys. A **34**, 1950195 (2019), arXiv:1808.10830 [hep-ph].
[25] A. Abdesselam *et al.* (Belle), in *10th International Workshop on the CKM Unitarity Triangle* (2019) arXiv:1903.03102 [hep-ex].
[26] R. Alonso, B. Grinstein, and J. Martin Camalich, Phys. Rev. Lett. **118**, 081802 (2017), arXiv:1611.06676 [hep-ph].
[27] R. Aaij *et al.* (LHCb), (2022), arXiv:2201.03497 [hep-ex].
[28] W. Detmold, C. Lehner, and S. Meinel, Phys. Rev. **D92**, 034503 (2015), arXiv:1503.01421 [hep-lat].
[29] Marco Pappagallo (LHCB deputy physics coordinator) private communication.
[30] U. Nierste, S. Trine, and S. Westhoff, Phys. Rev. D **78**, 015006 (2008), arXiv:0801.4938 [hep-ph].
[31] M. Tanaka and R. Watanabe, Phys. Rev. D **87**, 034028 (2013), arXiv:1212.1878 [hep-ph].
[32] S. Fajfer, J. F. Kamenik, and I. Nisandzic, Phys. Rev. **D85**, 094025 (2012), arXiv:1203.2654 [hep-ph].
[33] M. Duraisamy and A. Datta, JHEP **09**, 059 (2013), arXiv:1302.7031 [hep-ph].
[34] M. Duraisamy, P. Sharma, and A. Datta, Phys. Rev. D **90**, 074013 (2014), arXiv:1405.3719 [hep-ph].
[35] D. Becirevic, S. Fajfer, I. Nisandzic, and A. Tayduganov, Nucl. Phys. B **946**, 114707 (2019), arXiv:1602.03030 [hep-ph].
[36] Z. Ligeti, M. Papucci, and D. J. Robinson, JHEP **01**, 083 (2017), arXiv:1610.02045 [hep-ph].
[37] M. A. Ivanov, J. G. Körner, and C.-T. Tran, Phys. Rev. D **95**, 036021 (2017), arXiv:1701.02937 [hep-ph].
[38] F. U. Bernlochner, Z. Ligeti, M. Papucci, and D. J. Robinson, Phys. Rev. **D95**, 115008 (2017), [erratum: Phys. Rev.D97,no.5,059902(2018)], arXiv:1703.05330 [hep-ph].
[39] M. Blanke, A. Crivellin, S. de Boer, T. Kitahara, M. Moscati, U. Nierste, and I. Nišandžić, Phys. Rev. **D99**, 075006 (2019), arXiv:1811.09603 [hep-ph].
[40] S. Bhattacharya, S. Nandi, and S. Kumar Patra, Eur. Phys. J. C **79**, 268 (2019), arXiv:1805.08222 [hep-ph].
[41] P. Colangelo and F. De Fazio, JHEP **06**, 082 (2018), arXiv:1801.10468 [hep-ph].
[42] C. Murgui, A. Penuelas, M. Jung, and A. Pich, JHEP **09**, 103 (2019), arXiv:1904.09311 [hep-ph].

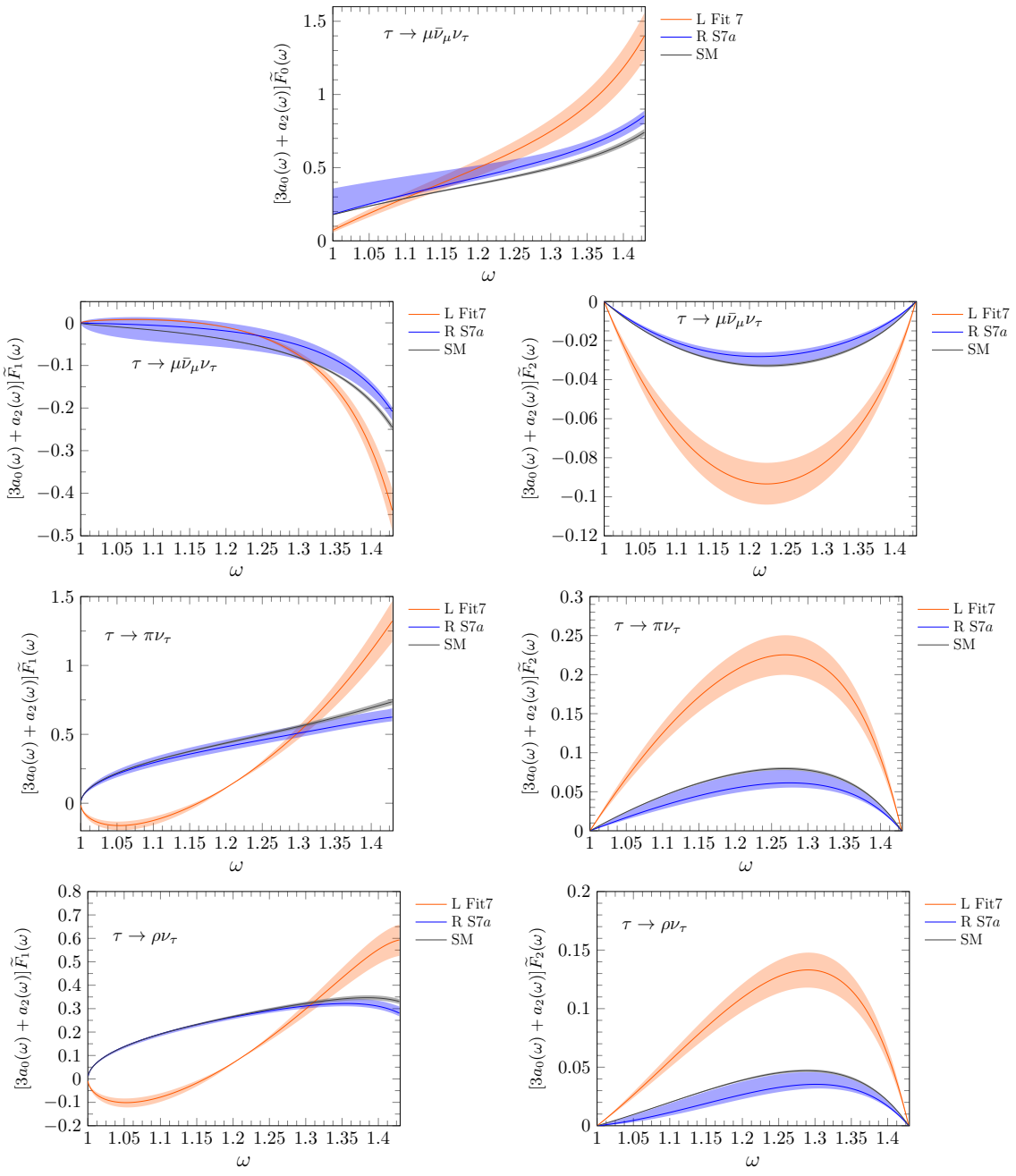

FIG. 7. Results for the functions $n_0(\omega)\widetilde{F}^d_{0,1,2}(\omega)$ evaluated for the $\bar{B} \to D\tau(\mu\bar{\nu}_\mu\nu_\tau, \pi\nu_\tau, \rho\nu_\tau)\bar{\nu}_\tau$ decays, keeping $y = m_{\mu,\pi,\rho}/m_\tau$ finite, and obtained within the SM and the beyond the SM scenarios of Fits 7 and 7a of Refs. [42] and [45], which only includes left- (right-)handed neutrino NP operators, respectively. Error bands account for uncertainties induced by both form-factors and fitted Wilson coefficients (added in quadrature).

[43] R.-X. Shi, L.-S. Geng, B. Grinstein, S. Jäger, and J. Martin Camalich, JHEP **12**, 065 (2019), arXiv:1905.08498 [hep-ph].

[44] A. K. Alok, D. Kumar, S. Kumbhakar, and S. Uma Sankar, Nucl. Phys. B **953**, 114957 (2020), arXiv:1903.10486 [hep-ph].

[45] R. Mandal, C. Murgui, A. Peñuelas, and A. Pich, JHEP **08**, 022 (2020), arXiv:2004.06726 [hep-ph].

[46] S. Kumbhakar, Nucl. Phys. B **963**, 115297 (2021), arXiv:2007.08132 [hep-ph].

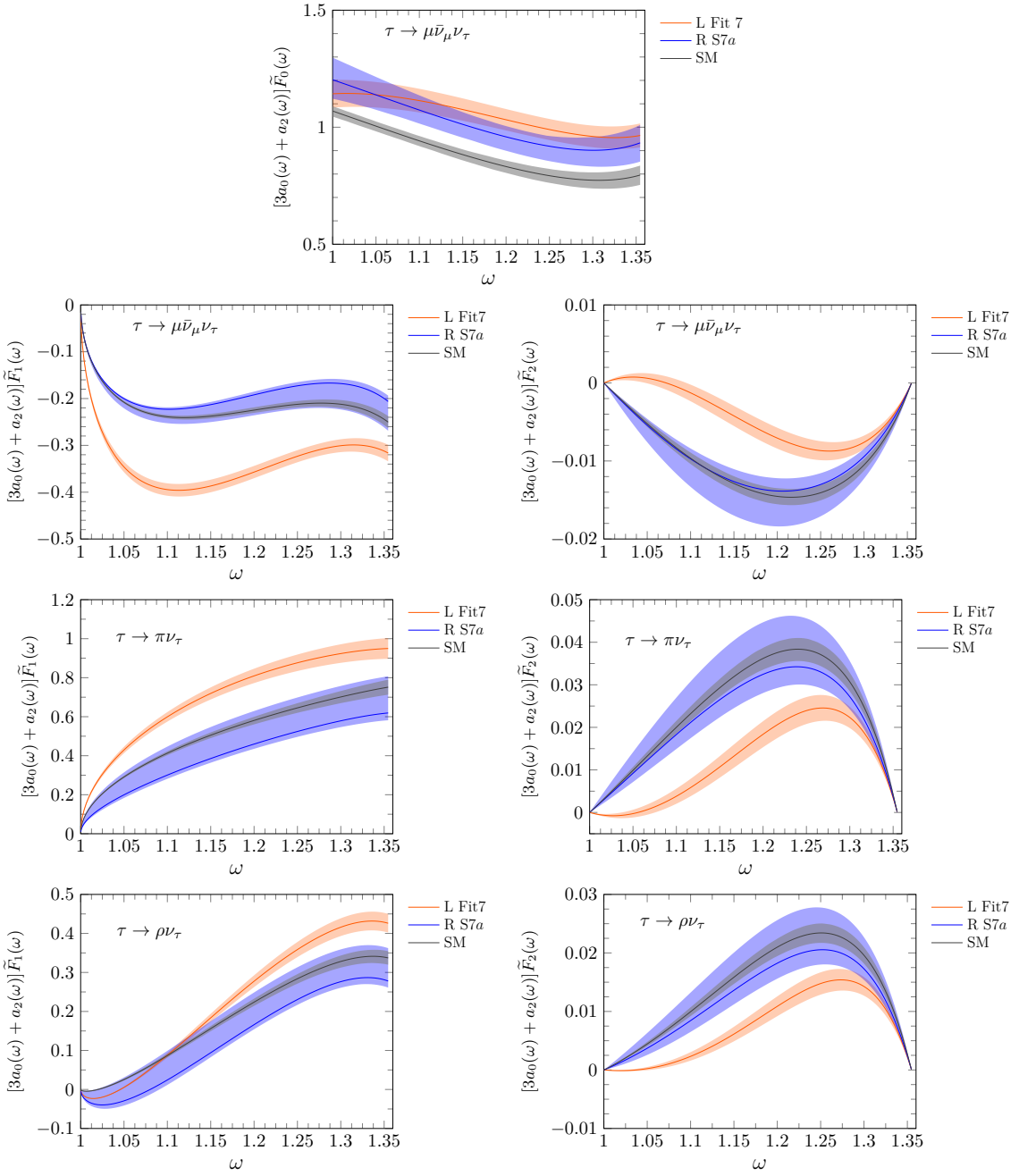

FIG. 8. Same as in Fig. 7, but for the $\bar{B} \to D^*\tau(\mu\bar{\nu}_\mu\nu_\tau, \pi\nu_\tau, \rho\nu_\tau)\bar{\nu}_\tau$ decays.

[47] S. Iguro and R. Watanabe, JHEP **08**, 006 (2020), arXiv:2004.10208 [hep-ph].
[48] B. Bhattacharya, A. Datta, S. Kamali, and D. London, JHEP **07**, 194 (2020), arXiv:2005.03032 [hep-ph].
[49] N. Penalva, E. Hernández, and J. Nieves, JHEP **06**, 118 (2021), arXiv:2103.01857 [hep-ph].
[50] N. Penalva, E. Hernández, and J. Nieves, Phys. Rev. D **102**, 096016 (2020), arXiv:2007.12590 [hep-ph].
[51] R. Dutta and A. Bhol, Phys. Rev. D **96**, 076001 (2017), arXiv:1701.08598 [hep-ph].
[52] J. Harrison, C. T. Davies, and A. Lytle (LATTICE-HPQCD), Phys. Rev. Lett. **125**, 222003 (2020), arXiv:2007.06956 [hep-lat].
[53] R. Dutta, Phys. Rev. D **93**, 054003 (2016), arXiv:1512.04034 [hep-ph].
[54] S. Shivashankara, W. Wu, and A. Datta, Phys. Rev. D **91**, 115003 (2015), arXiv:1502.07230 [hep-ph].

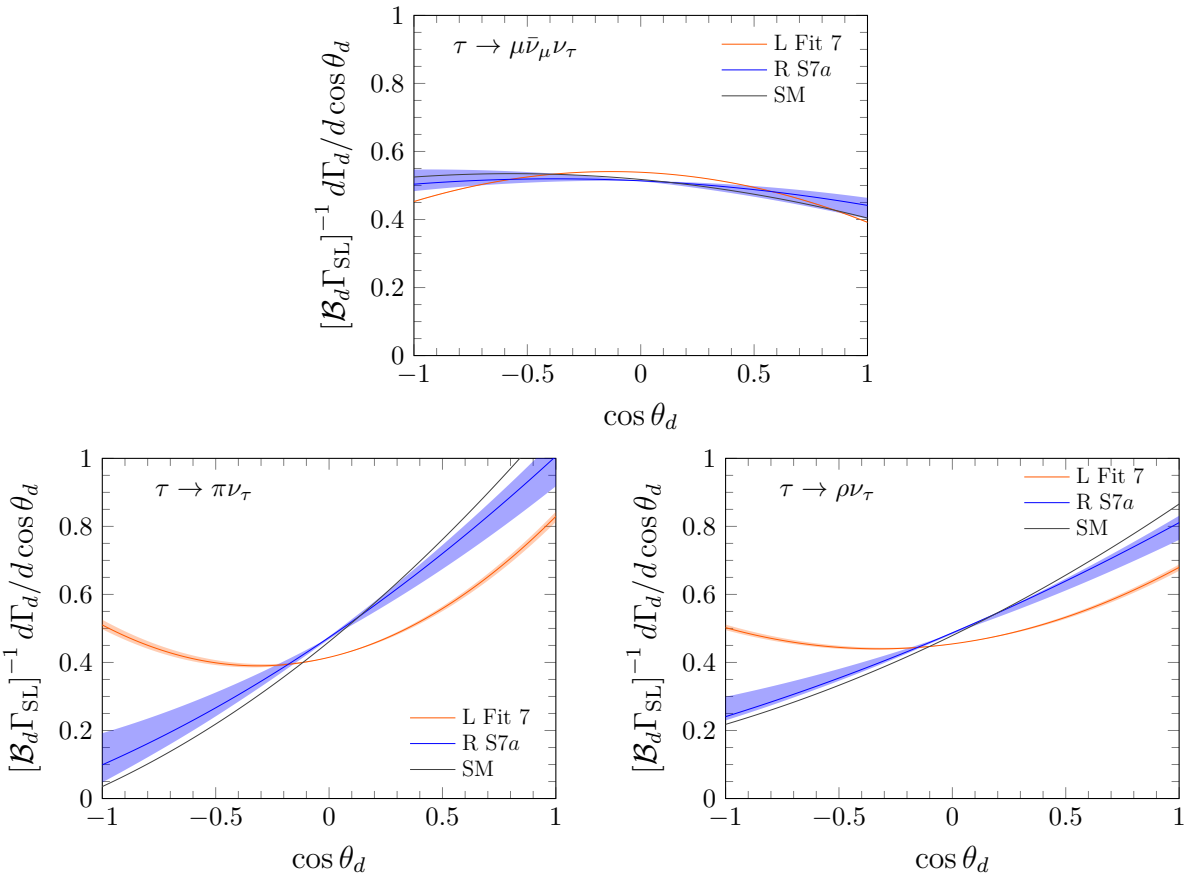

FIG. 9. Angular $d\Gamma/d\cos\theta_d$ distribution for the $\bar{B} \to D\tau(\mu\bar{\nu}_\mu\nu_\tau, \pi\nu_\tau, \rho\nu_\tau)\bar{\nu}_\tau$ decays, keeping $y = m_d/m_\tau$ to its finite value, and obtained within the SM and the beyond the SM scenarios of Fits 7 and 7a of Refs. [42] and [45], which only includes left- (right-)handed neutrino NP operators, respectively. Details as in Fig. 5.

[55] X.-Q. Li, Y.-D. Yang, and X. Zhang, JHEP **02**, 068 (2017), arXiv:1611.01635 [hep-ph].
[56] A. Datta, S. Kamali, S. Meinel, and A. Rashed, JHEP **08**, 131 (2017), arXiv:1702.02243 [hep-ph].
[57] A. Ray, S. Sahoo, and R. Mohanta, Phys. Rev. **D99**, 015015 (2019), arXiv:1812.08314 [hep-ph].
[58] F. U. Bernlochner, Z. Ligeti, D. J. Robinson, and W. L. Sutcliffe, Phys. Rev. **D99**, 055008 (2019), arXiv:1812.07593 [hep-ph].
[59] E. Di Salvo, F. Fontanelli, and Z. J. Ajaltouni, Int. J. Mod. Phys. **A33**, 1850169 (2018), arXiv:1804.05592 [hep-ph].
[60] M. Blanke, A. Crivellin, T. Kitahara, M. Moscati, U. Nierste, and I. Nišandžić, Phys. Rev. **D100**, 035035 (2019), arXiv:1905.08253 [hep-ph].
[61] P. Böer, A. Kokulu, J.-N. Toelstede, and D. van Dyk, (2019), arXiv:1907.12554 [hep-ph].
[62] X.-L. Mu, Y. Li, Z.-T. Zou, and B. Zhu, Phys. Rev. D **100**, 113004 (2019), arXiv:1909.10769 [hep-ph].
[63] Q.-Y. Hu, X.-Q. Li, Y.-D. Yang, and D.-H. Zheng, JHEP **02**, 183 (2021), arXiv:2011.05912 [hep-ph].
[64] N. Penalva, E. Hernández, and J. Nieves, Phys. Rev. **D100**, 113007 (2019), arXiv:1908.02328 [hep-ph].
[65] N. Penalva, E. Hernández, and J. Nieves, Phys. Rev. D **101**, 113004 (2020), arXiv:2004.08253 [hep-ph].
[66] R. Alonso, A. Kobach, and J. Martin Camalich, Phys. Rev. D **94**, 094021 (2016), arXiv:1602.07671 [hep-ph].
[67] R. Alonso, J. Martin Camalich, and S. Westhoff, Phys. Rev. D **95**, 093006 (2017), arXiv:1702.02773 [hep-ph].
[68] P. Asadi, A. Hallin, J. Martin Camalich, D. Shih, and S. Westhoff, Phys. Rev. D **102**, 095028 (2020), arXiv:2006.16416 [hep-ph].

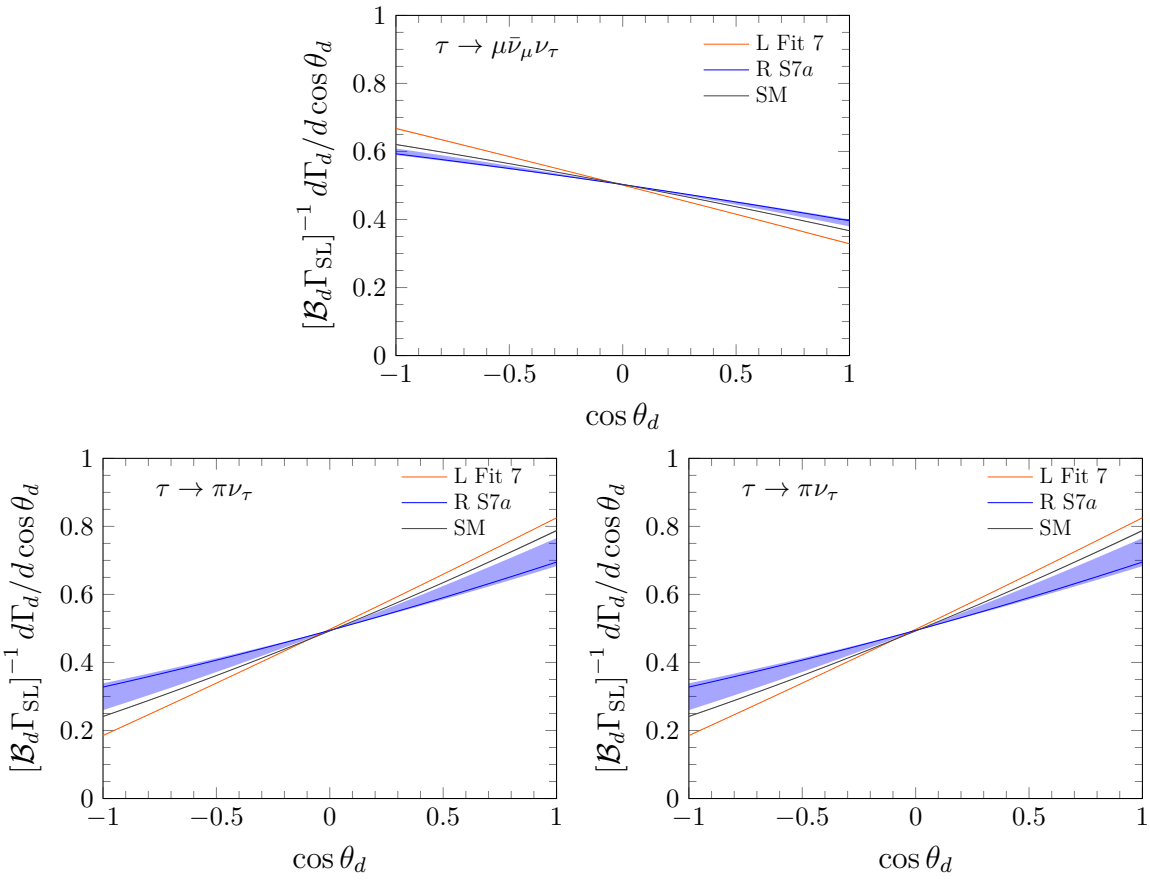

FIG. 10. Same as in Fig. 9, but for the $\bar{B} \to D^*\tau(\mu\bar{\nu}_\mu\nu_\tau, \pi\nu_\tau, \rho\nu_\tau)\bar{\nu}_\tau$ decays.

[69] N. Penalva, E. Hernández, and J. Nieves, JHEP **10**, 122 (2021), arXiv:2107.13406 [hep-ph].

[70] M. Tanaka and R. Watanabe, Phys. Rev. D **82**, 034027 (2010), arXiv:1005.4306 [hep-ph].

[71] A. Cerri *et al.*, "Report from Working Group 4: Opportunities in Flavour Physics at the HL-LHC and HE-LHC," in *Report on the Physics at the HL-LHC,and Perspectives for the HE-LHC*, Vol. 7, edited by A. Dainese, M. Mangano, A. B. Meyer, A. Nisati, G. Salam, and M. A. Vesterinen (2019) pp. 867–1158, arXiv:1812.07638 [hep-ph].